

RIGA TECHNICAL UNIVERSITY

Faculty of Electronics and Telecommunications
Institute of Telecommunications

Uģis Senkāns

Doctoral Student of the Study Programme “Telecommunications”

**DEVELOPMENT AND EVALUATION OF
HYBRID FBG SENSORS AND WDM-PON FIBER
OPTICAL SYSTEMS**

Summary of the Doctoral Thesis

Scientific Supervisors
Professor Dr. sc. ing.
SANDIS SPOLĪTIS

Professor Dr. sc. ing.
VJAČESLAVS BOBROVS

RTU Press
Riga 2021

Seņkāns, U. Development and Evaluation of Hybrid FBG Sensors and WDM-PON Fiber Optical Systems. Summary of the Doctoral Thesis. – Riga: RTU Press, 2021, – 39 p.

Published in accordance with the decision of the Promotion Council “RTU P-08” of 11 October 2021, Minutes No. 3.

The research was supported by the European Social Fund within the project “Strengthening of the academic staff of Riga Technical University in the fields of strategic specialization” No. 8.2.2.0/18/A/017.

NATIONAL
DEVELOPMENT
PLAN 2020



EUROPEAN UNION
European Social
Fund

INVESTING IN YOUR FUTURE

<https://doi.org/10.7250/9789934227004>

ISBN 978-9934-22-700-4 (pdf)

DOCTORAL THESIS PROPOSED TO RIGA TECHNICAL UNIVERSITY FOR THE PROMOTION TO THE SCIENTIFIC DEGREE OF DOCTOR OF SCIENCE

To be granted the scientific degree of Doctor of Science (Ph. D.), the present Doctoral Thesis has been submitted for the defence at the open meeting of RTU Promotion Council on December 17, 2021 at the Faculty of Electronics and Telecommunications of Riga Technical University, 12 Azenes Str.2, Room 201.

OFFICIAL REVIEWERS

Associate Professor Dr. sc. ing. Aleksandrs Ipatovs
Riga Technical University

Senior Researcher Dr. sc. ing. Xiaodan Pang
KTH Royal Institute of Technology, Sweden

Leading Researcher Dr. habil. sc. ing. Manfreds Šnepš-Šneppe
Ventspils University of Applied Sciences, Latvia

DECLARATION OF ACADEMIC INTEGRITY

I hereby declare that the Doctoral Thesis submitted for review to Riga Technical University for the promotion to the scientific degree of Doctor of Science (Ph. D.) is my own. I confirm that this Doctoral Thesis has not been submitted to any other university for promotion to a scientific degree.

Uģis Senkāns (signature)

Date:

The Doctoral Thesis has been written in Latvian. It consists of an introduction; 4 Chapters; Conclusions; 55 figures; 1 appendix; the total number of pages is 127. The Bibliography contains 176 titles.

ACKNOWLEDGMENT

I would like to thank my Ph. D. supervisors Professor Sandis Spolītis and Professor Vjačeslavs Bobrovs for their valuable advice, suggestions, and support throughout the doctoral study program, as well as the development of the Doctoral Thesis.

Thanks to my colleagues Jānis Braunfelds and Toms Salgals, with whom I had the honor to work together during my doctoral studies. Thank you for the support and advice that contributed to this work.

My heartfelt thanks to my wife Līva and my entire family, without whose help, understanding, and love I would not have succeeded. Your support is invaluable.

Thank you to everyone I have worked with or who has supported me but whose name is not mentioned here.

GENERAL DESCRIPTION OF THE RESEARCH

Topicality of the Research

The world is currently experiencing rapid development and convergence of telecommunications technologies into converged data transmission and sensor systems. With the development of fiber optic data transmission technologies and infrastructure on a global scale, the use of fiber optic sensors to perform sensor functions is becoming increasingly important. Therefore, to ensure more efficient use of optical sensor technologies, it is necessary to research and search for new solutions for the integration and use of fiber optic sensors in the existing and future architecture of optical metro-access communication systems.

The volume of optical data transmission information is growing faster and faster every year, as evidenced by Cisco, one of the world's largest and leading manufacturers of telecommunications network equipment. Over the last 5 years, total internet traffic has increased by at least 30 %, since more and more devices are interconnected and more and more information is consumed. Figure 1 shows the global amount of exabytes consumed per month over several years, as well as the forecast for the next 2 years [38].

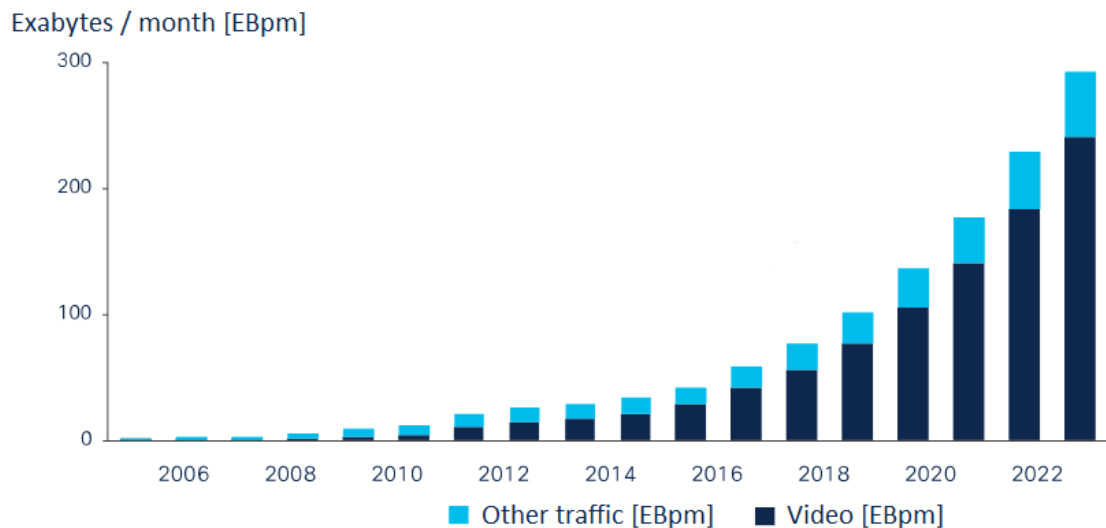


Fig. 1. Monthly global consumption of optical network data [38].

Globally, the total number of Internet users is projected to increase from 3.8 billion in 2018 to 5.3 billion in 2023. In terms of population, these figures represent 51 % of the world's population in 2018 and 66 % of the world's population in 2023 [37].

Optical network data is growing, and so do related technologies, their amount and ability to combine these technologies with fiber-optic transmission infrastructure. One of such technologies, that has a growing demand, is fiber optic sensors. Recent survey and forecast data published by research institutions, such as *Grand View Research* [42] in December 2019 and *Global market Insights* [41] in December 2020 show that the global compound annual growth rate of fiber optic sensor technology (CAGR) is more than 10 %, which means that the average annual growth of the optical sensor market will continue to increase in the near future (at least until 2025–2026).

The rapid development of modern information transmission technologies and fiber optic communication networks is essential for the research, improvement, and development of fiber optic sensors. When comparing fiber optic sensors with their predecessor technology, traditional electrical and mechanical sensors, it is important to emphasize the unique advantages of fiber optic sensors, such as lightweight, multiplexing capabilities, small size, and others. This

technology makes it possible to place, for instance, several fiber Bragg grating (FBG) optical sensors on one optical fiber. They also have resistance to corrosion and electromagnetic interference. Due to their significant advantages, optic sensors can be used effectively to monitor transport and construction infrastructure worldwide. Thus, the overall infrastructure costs and the overall efficiency of the industry can be significantly improved [7], [19], [33].

The research of fiber optic sensors is performed in the dissertation, with special emphasis on FBG temperature and strain optical sensors, as well as the integration of fiber optic sensor network in WDM passive optical network (PON) metro access systems. To evaluate the performance of such unified systems, a study of the interaction between the FBG optical sensor network and the fiber optic data transmission system has been performed. Also, the FBG sensor network has been implemented in a spectrally sliced WDM-PON transmission system, where only one incoherent broadband light source is used as the light source on all network terminals.

The Aims and Tasks of the Thesis

Summing up the aforementioned facts, the **aim of the Doctoral Thesis** is to carry out theoretical and experimental research and evaluation of the interaction of FBG fiber optic sensor networks and WDM-PON metro-access transmission systems implemented in a single system.

To achieve the aim, it is necessary to perform the following **key tasks**:

1. To study the principles of manufacturing fiber optical sensors, technological development, division according to the principle of their operation and application based on the analysis of scientific literature.
2. To perform compatibility assessment of fiber FBG optical sensor network with WDM-PON fiber optic metro-access transmission system infrastructure.
3. To develop a simulation model of a combined up to 5 FBG temperature sensor system and a dense 10 Gbit/s WDM-PON transmission system, to evaluate their collaboration and to study the effect of measured temperature on the changes of the reflected wavelength of FBG optical sensors in such a system.
4. To develop an algorithm for processing the spectral peaks of the reflected signals of advanced precision FBG sensors and to study the minimum allowable channel spacing of such optical sensors in a combined 5 FBG sensor and 8-channel 10 Gbit/s WDM-PON transmission system.
5. To evaluate the performance of a hybrid, up to 10 Gbit/s simulation scheme by creating a hidden 7-channel spectrally sliced data transmission system and combine it with an 8-channel WDM-PON data transmission system with an integrated 5 optical sensor system.
6. Experimentally and in a simulation environment to develop and evaluate a combined FBG optical sensor and a spectrally sliced 1.5 Gbit/s fiber optic metro-access transmission system model, where one shared broadband light source is used as the light source.

The Research Methods

Mathematical calculations, numerical simulations, and experimental measurements have been used in realization of the tasks set in the dissertation and the analysis of problems. RSoft Optsim simulation software and Mathworks MATLAB numerical calculation software were used for the realization of DWDM-PON, WDM-PON, and spectrally sliced SS-WDM PON systems, as well as FBG fiber optic sensor network. Several research methods have been used in the work, such as approximation, time domain split-step method, Monte Carlo method (for estimating the bit error rate (BER)), as well as individual signal processing algorithms developed by the author. Measurements of signal power, spectrum, eye diagrams, and bit errors were used to evaluate the quality of optical sensors and data signals. The scientific experiments

included in the dissertation have been carried out in the Scientific Laboratory of Fiber Optic Transmission Systems (ŠOPS) of the Communication Systems Technology Research Center (SSTIC) of the Riga Technical University (RTU) Telecommunications Institute (TI).

Research Results

Novel achievements and practical value of the Doctoral Thesis are as follows:

1. A model of a combined FBG fiber optic temperature sensor network and wavelength division multiplexed fiber optic metro-access data transmission system has been developed, as well as the effect of the measured temperature impact on the changes of the reflected wavelength of FBG optical sensors has been determined.
2. The minimum allowable optical sensor channel spacings are calculated in the network of 5 FBG optical sensors and 8-channel 10 Gbit/s WDM-PON data transmission system, for operation in the optical C-band (1530–1565 nm).
3. A mathematical algorithm has been developed, which provides the possibility to determine the minimum allowable channel spacing of FBG optical sensors, as well as the reflected signal processing algorithm, which allows to more accurately determine the reflected spectral peaks of FBG optical sensors' signals.
4. A simulation model and experimental layout of a spectrally sliced 10 Gbit/s WDM-PON 32 data channel transmission system and an FBG optical sensor network have been developed, where one shared broadband light source is used as the light source.
5. A common system model has been developed, in which a network of 5 FBG optical sensors together with 8 WDM-PON 10 Gbit/s transmission data channels are located within one optical fiber, between which a system of 7 data transmission channels with a transmission speed of 2.5 Gbit/s is hidden.

During the development of the Doctoral Thesis, the following **main conclusions** were obtained:

1. The developed hybrid system's model, which includes a network of 5 FBG fiber optic temperature sensors and 4 data channels, 10 Gbit/s WDM-PON fiber optic metro-access communication system, can provide at least 20 km long data transmission line operation with accepted received BER signal of $\leq 10^{-9}$ and determine the effect of the measured temperature on the variation of the reflected wavelength of the FBG optical sensors, which in this configuration is on average 1 GHz (8 pm) per 1 °C.
2. With the advanced precision FBG sensors' reflected signal spectral peak algorithm and mathematical equation developed in this work, it is possible to calculate and estimate the FBG optical sensors' theoretical channel spacing in the FBG sensors' network, which in the optical C-band (frequency range from 192 THz to 195.5 THz) is at least 207.746 GHz.
3. Using a single shared broadband light source, a combined spectrally sliced 1.5 Gbit/s 32 data channel WDM-PON transmission and FBG optical sensor network model can be created, providing the received BER of the data signal $\leq 9.7 \times 10^{-12}$ in B2B (no fiber optic line) configuration and $\text{BER} \leq 6.1 \times 10^{-7}$ in a 20 km long transmission line configuration.
4. Within one optical fiber, a model can be created in which a network of 5 FBG optical sensors is placed together with 8 WDM-PON 10 Gbit/s transmission data channels, between which a 2.5 Gbit/s 7 data channel system is visually hidden, ensuring adequate received signal quality ($\text{BER} \leq 7.16 \times 10^{-17}$ for the WDM-PON system and $\text{BER} \leq 1.11 \times 10^{-5}$ for the stealth data channel system) after a 20 km long fiber optic data transmission line.

Thesis Statements to Be Defended:

1. It is possible to develop a hybrid 5 FBG fiber optic temperature sensor and 4 wavelength division multiplexed 10 Gbit/s data transmission channel metro-access system using a 20 km long transmission line, where the received signal's BER $< 10^{-9}$, as well as to determine the temperature's measured effect on the changes in the reflected wavelength of the FBG optical sensor, averaging 1 GHz (8 pm) per 1 °C in this configuration.
2. Using the advanced precision FBG sensor reflected signal spectral peak processing algorithm, as well as mathematical equation that is developed in this work, it is possible to calculate FBG optical sensors' theoretical channel spacing in fiber optic FBG sensor network, knowing the predicted range of measured object or ambient temperature change/wavelength shift as well as the average spectral bandwidth of the FBG optical sensor's reflected signal in a power drop zone of -7 dB.
3. The minimum allowable channel spacing of optical sensors in a combined 5 FBG optical sensor and 8-channel 10 Gbit/s WDM-PON data transmission system network, in the optical C-band, in the frequency range from 192.0 THz to 195.5 THz has to be at least 207.746 GHz.
4. In the combined FBG sensor and WDM metro-access communication system, using a single shared broadband light source, it is possible to ensure both stable operation of the FBG optical sensor and operation of spectrally sliced 32 data transmission channels with a transmission speed of 1.5 Gbit/s, ensuring the received signal BER at least below the 2×10^{-3} threshold in an optical transceiver using forward error correction (FEC).
5. Between eight 10 Gbit/s WDM-PON system channels, using two additional incoherent broadband light sources, where the optical spectrum generated by one light source is cut into 7 slices and used for data transmission at a speed of 2.5 Gbit/s per channel, and the other – for placement of 5 optical sensors, it is possible to hide these spectrally sliced channels, which are not visible in the optical spectrum when connecting to the ODN section and the end-user (ONT) side of the optical transmission line. Operation of such a system with BER below the 2×10^{-3} FEC threshold is feasible at a fiber optic transmission line length of at least 20 km.

Approbation of Research Results

The main results of the Doctoral Thesis have been presented at 5 international scientific conferences, reported in 4 publications in scientific journals, 5 publications in full-text conference proceedings. The recommendations developed in the work are intended both for the improvement of the existing optical metro-access networks as well as for the introduction of new fiber optic transmission systems and sensor networks.

Reports at the scientific conferences:

1. April 23, 2020 – Participation in **RTU 61st student scientific and technical conference** with presentation “WDM-PON and data transmission of optically hidden signals for steganography purposes”.
2. October 15, 2019 – Participation in **RTU 60th student scientific and technical conference** with presentation “Unified Multi-channel Spectrum-sliced WDM-PON Transmission System with Embedded FBG Sensors Network”.
3. November 16, 2018 – Participation in the **international conference “Advances in Wireless and Optical Communications, RTUWO’18”** with presentation “Research of FBG Optical Sensors Network and Precise Peak Detection”.
4. October 12, 2018 – Participation in **RTU 59th student scientific and technical conference** with presentation “Research of FBG Optical Sensors Network and Precise Peak Detection”.

5. November 3, 2017 – Participation in the **international conference “Advances in Wireless and Optical Communications, RTUWO’17”** with presentation “Evaluation and Research of FBG Optical Temperature Sensors Network”.
6. October 13, 2017 – Participation in **RTU 58th student scientific and technical conference** with presentation “Optical fiber temperature sensor functionality research and experimental analysis”.
7. April 29, 2017 – Participation with the Master's thesis in the **57th RTU student scientific and technical conference**.

Publications in scientific journals:

1. Supe, A., Olonkins, S., Udalcovs, A., Senkans, U., Mūrnieks, R., Gegere, L., Prigunovs, D., Grube, J., Elsts, E., Spolītis, S., Ozolins, O., Bobrovs, V., “**Cladding-Pumped Erbium/Ytterbium Co-Doped Fiber Amplifier for C-Band Operation in Optical Networks**”. *Applied Sciences*. 2021; 11(4):1702. <https://doi.org/10.3390/app11041702>
2. Braunfelds, J., Senkans, U., Skels, P., Janeliukstis, R., Salgals, T., Redka, D., Lyashuk, I., Porins, J., Spolītis, S., Haritonovs, V., Bobrovs, V., “**FBG-Based Sensing for Structural Health Monitoring of Road Infrastructure**”, *Journal of Sensors*, vol. 2021, Article ID 8850368, 11 pages, 2021. <https://doi.org/10.1155/2021/8850368>
3. Senkāns, U., Bobrovs, V., Ivanovs, Ģ., Spolītis, S. “**Research of Hybrid WDM-PON Data Transmission System with Embedded ASE-Powered Stealth Channels for Steganography Applications**”. *Optical Fiber Technology*, 2020, Vol. 58, pp. 1–8. ISSN 1068-5200. Available from: doi:10.1016/j.yofte.2020.102300
4. Senkāns, U., Braunfelds, J., Lyashuk, I., Poriņš, J., Spolītis, S., Bobrovs, V. “**Research on FBG Based Sensor Networks and Their Coexistence with Fiber Optical Transmission Systems**”. *Journal of Sensors*, 2019, Vol. 2019, pp. 1–13. ISSN 1687-725X. e-ISSN 1687-7268. Available from: doi:10.1155/2019/6459387

Publications in full-text conference proceedings:

1. Supe, A., Spolītis, S., Elsts, E., Mūrnieks, R., Doke, G., Senkāns, U., Matsenko, S., Grube, J., Bobrovs, V. “**Recent Developments in Cladding-Pumped Doped Fiber Amplifiers for Telecommunications System**”. In: *Proceedings of 22nd International Conference on Transparent Optical Networks (ICTON 2020)*, Italy, Bari, 19–23 July 2020. Piscataway: IEEE, 2020, pp. 1–6.
2. Senkāns, U., Braunfelds, J., Lyashuk, I., Poriņš, J., Spolītis, S., Haritonovs, V., Bobrovs, V. “**FBG Sensors Network Embedded in Spectrum-sliced WDM-PON Transmission System Operating on Single Shared Broadband Light Source**”. In: *Proceedings of Photonics & Electromagnetics Research Symposium (PIERS 2019)*, China, Xiamen, 17–20 December 2019. Piscataway: IEEE, 2019, pp. 1–9.
3. Braunfelds, J., Senkāns, U., Lyashuk, I., Poriņš, J., Spolītis, S., Bobrovs, V. “**Unified Multi-channel Spectrum-sliced WDM-PON Transmission System with Embedded FBG Sensors Network**”. In: *Proceedings of Photonics & Electromagnetics Research Symposium (PIERS 2019)*, Italy, Rome, 17–20 June 2019. Piscataway: IEEE, 2019, pp. 1–7.
4. Senkāns, U., Braunfelds, J., Spolītis, S., Bobrovs, V. “**Research of FBG Optical Sensors Network and Precise Peak Detection**”. In: 2018 Advances in Wireless and Optical Communications (RTUWO 2018): Proceedings, Latvia, Riga, 15–16 November 2018. Piscataway: IEEE, 2018, pp. 139–143. ISBN 978-1-5386-5559-7. e-ISBN 978-1-5386-5558-0. Available from: doi:10.1109/RTUWO.2018.8587859

5. Senkāns, U., Spoļītis, S., Bobrovs, V. Evaluation and “**Research of FBG Optical Temperature Sensors Network**” In: *2017 Advances in Wireless and Optical Communications (RTUWO 2017): Proceedings*, Latvia, Riga, 2–3 November 2017. Piscataway: IEEE, 2017, pp. 79–89. ISBN 978-1-5386-0586-8. e-ISBN 978-1-5386-0585-1. Available from: doi:10.1109/RTUWO.2017.8228509

The results obtained during the Doctoral Thesis have been used in 2 scientific research projects.

International scientific research projects:

1. ESF project “To strengthen academic staff of higher education institutions in strategic specialization areas”, No. 8.2.2.0/18/A/017.
2. ERAF project “Effective Stockpile Pumped Fiber Optical development of amplifiers for telecommunication systems”, No. 1.1.1.1/18/A/068.

Volume and Structure of the Doctoral Thesis

The volume of the Doctoral Thesis is 127 pages. It consists of an introduction, four chapters, a bibliography, and 1 appendix.

In Chapter 1, the operation types and classification of fiber optic sensors are evaluated by analyzing wavelength modulated, phase modulated, intensity modulated and polarization modulated optical sensors. A classification study of the application of fiber optic sensors has been performed, especially focusing on the FBG optical sensors. The application of fiber optic sensors for the needs of IoT and SHM is analyzed, as well as the trends in the consumption of data volume transmitted by fiber optic transmission systems in modern society are considered. The aim of the dissertation, tasks to reach the aim, new scientific acquisitions, theses to be defended, as well as the main results are formulated in the chapter.

In Chapter 2, the development of a network of 5 fiber optical FBG temperature sensors have been implemented and combined with four 10 Gbit/s data channel DWDM-PON transmission system. The selection and creation of the parameters of the components included in the transmitter side and the optical line terminal are analyzed. The selection and development of the parameters of the optical distribution network and fiber optic sensor network as well as the development of the receiver side of the communication system and the implementation of optical sensor signal processing are also studied. As a result, the effect of the measured temperature on the changes in the reflected wavelength of the FBG optical sensors (approximately 1 GHz to 1 °C) has been determined.

In Chapter 3, the study of the interaction of 5 FBG optical sensors’ network and 10 Gbit/s WDM-PON fiber optical 8 data channel transmission system in a 20 km long transmission line is developed and analyzed. An advanced precision algorithm for processing the spectral peaks of the reflected signals of FBG sensors has been developed. Within the framework of this co-operation system model, a mathematical equation has been developed, which determines the minimum allowable channel spacing between optical channels (~208 GHz). Further in this chapter, the development of a hybrid 10 Gbit/s WDM 8 data channel communication system, 2.5 Gbit/s 7 hidden data channels, and a 5-fiber optical sensor network on a 20 km long transmission line, which is useful for steganography, is discussed. An evaluation of the visualization of the spectral characteristics obtained by this developed model as well as a performance analysis has been performed.

In Chapter 4, the development of a simulation model is created and analyzed – the implementation of a 7 FBG sensors network in a spectrally sliced WDM-PON 32 data channel transmission system, which works with a single shared broadband light source in various scenarios. Performance analysis of the developed 2.5 Gbit/s and 10 Gbit/s spectrally sliced

WDM-PON system in a 28 km long transmission line model with and without integrated 7 FBG fiber optic network was performed. Further in this chapter, the joint architecture development of a simulation and experimental model is considered by studying the 1.25 Gbit/s and 1.5 Gbit/s spectrally sliced WDM-PON 32 data channel fiber optic transmission system based on a single broadband light source (B2B and 20 km long transmission line) with integrated FBG optical sensor.

The Doctoral Thesis is concluded with substantiated and summarized main conclusions obtained during the research. Lists of publications, conferences, and projects are presented in the appendix.

SUMMARIES OF CHAPTERS OF THE DOCTORAL THESIS

Chapter 1

In this chapter, the evaluation of the operation types and classification of fiber optic sensors is performed, as well as the application of the fiber Bragg grating in the implementation of fiber optic sensors is investigated.

Fiber optic sensors can be used for a variety of measurements, but there are key physical parameters that are both measured and constantly monitored, such as strain, temperature, gas consistency, resistance, the vibration of mechanisms and structures, distance between stationary and moving components, electrical current, high voltage, pressure, and others [3], [4], [18], [27].

When developing fiber optic sensors, several implementation variants are possible. One of the relatively easiest ways to measure the amplitude of light during measurements is to provide an amplitude modulated sensor. Sensors of this type were standard in the initial production of fiber optic sensors, however, over time, they were replaced by optical sensors based on wavelength modulation changes. This type of change was mainly based on the fact that wavelength change type sensors are much more stable and calibrated already during the production process. This can be explained by the fact that the losses caused by the connectors, the modal changes, as well as the changes in the lasers themselves or the aging of their technological life cycle do not directly affect the changes in the wavelength [18], [39].

A more detailed analysis of the operation of fiber optic sensors shows that there are many different types of fiber optic sensors, so their classification needs to be done. Primarily, it is possible to divide them into two main groups – external sensors (extrinsic) and internal sensors (intrinsic). Looking at the use of external sensors, it can be seen that the optical fiber in this situation is used as a signal transmission medium to be able to transmit a signal containing information data – an optical signal to or from an external system.

In turn, in the implementation of internal optical sensors, the optical signal may not leave the optical fiber to provide sensor functions. Types of internal sensors are selected, used, and researched more frequently, given their many advantages over external types of optical sensors. An example is the adaptation of their design to the receiving part of the sensor. By further exploring the distribution of classifications, depending on which elements are transformed and modified, fiber optic sensors can be divided into four more detailed categories [25]:

- 1) wavelength modulated (spectrometric) sensors;
- 2) phase modulated (interferometric) sensors;
- 3) intensity modulated sensors;
- 4) polarization modulated (polarimetric) sensors.

In addition to these categories, fiber optic sensors can also be divided by their measurement types as well as spatial location. A more detailed breakdown is shown in Fig. 2.

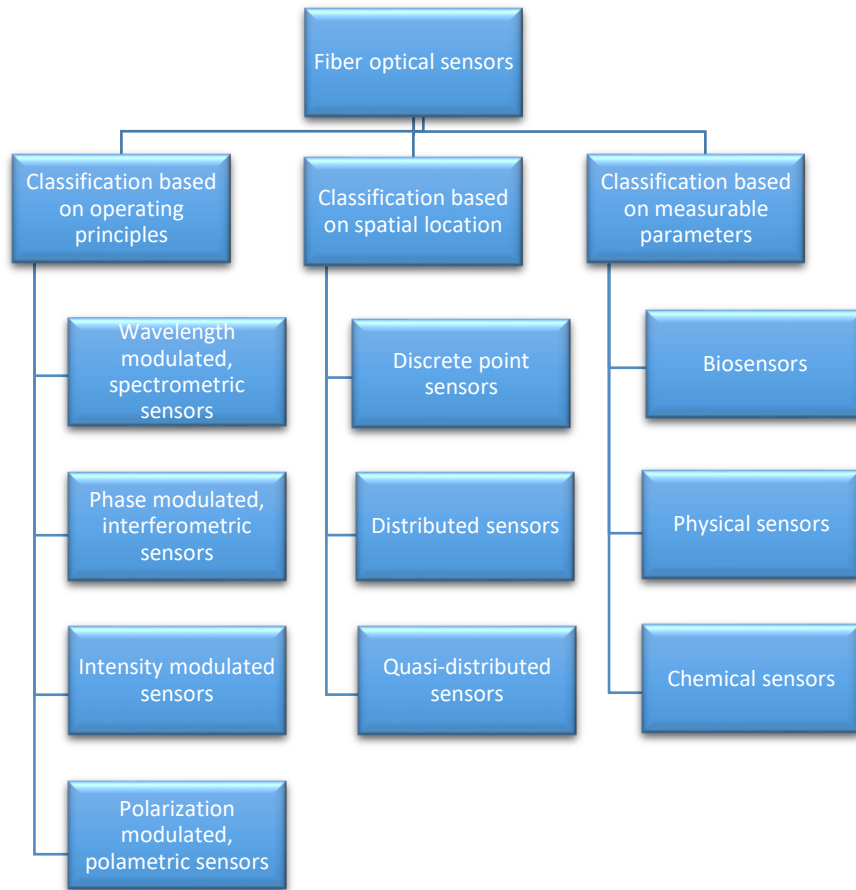


Fig. 2. Classification of fiber optic sensors [25].

Fiber optic sensors are used in various types of composite structures to provide versatile data – vibration measurement, temperature monitoring, treatment process information monitoring, as well as deformation, cracks, and other characteristics. The implementation of this type of measurement is closely related when directly and for calibration purposes performing measurements of strain, temperature or both parameters.

The disadvantage of this type of measurement is that the optical strain sensors of fibers are sensitive to changes in temperature and strain (study [1] indicates that the measurement error of FBG optical sensor in composite materials within one standard deviation is $\pm 62 \mu\epsilon$ in deformation measurements and $\pm 1.94 \text{ }^\circ\text{C}$ in temperature measurements). An effective way to ensure that these parameters are successfully separated is through the use of a fiber shield. This, in turn, makes it possible to implement optical sensors that are temperature insensitive (0.01 nm accuracy, observing the effect of temperature crossed sensitivity in the temperature range 5-60 $^\circ\text{C}$ [34]) or strain insensitive (achieving high sensitivity temperature detection – 106.64 pm/ $^\circ\text{C}$ in the temperature range from 200 $^\circ\text{C}$ to 1000 $^\circ\text{C}$, with a low cross-sensitivity effect of 0.00675 $^\circ\text{C}/\mu\epsilon$ [35]), thus significantly improving the accuracy of the data of the desired and measured parameter.

Temperature-based optical sensors can be used in a variety of industries, such as aerospace [13], medicine [22], maritime [2], and others. They can be used for high temperature measurements (above 1000 $^\circ\text{C}$) [31]. Fiber optic temperature sensor solutions can be adapted to provide very high sensitivity (21.86 pm/ $^\circ\text{C}$ [24], 24.68 pm/ $^\circ\text{C}$ [32], and even 2.16 nm/ $^\circ\text{C}$ [16], as well as 21.2 nm/ $^\circ\text{C}$ [9]). One example is the solution for long-distance (>100 km) optical fiber sensors, for example, in oil pipeline leak detection systems.

To date, various fiber optic type sensors have been developed, which can be classified as mentioned above. Nonetheless, some are selected more often than others, such as sensors

based on strain and temperature measurements. One of these types of optical sensors are sensors of fiber Bragg grating technology, which are used due to their relatively simple production and strong reflected signal (typically >95 % threshold is mentioned for high reflectance optical sensors [43]). From a terminological point of view, the definition of the Bragg grating is derived from Bragg's law and applied to periodic structures in the telecommunications fiber sector [18]. Bragg's law, defined in physical science, determines the relationship between the spacing of atomic planes in crystals and the angles of incidence at which these planes produce the most intense electromagnetic radiation, such as X-rays and gamma rays. In the mathematical equation of Bragg's law

$$n\lambda = 2d\sin\theta, \quad (1)$$

n is the number of light beams observed, λ is the wavelength, d is the distance between successive layers or planes of atoms, and θ is the angle of the incident or reflected light beam [36].

Further see the Bragg wavelength formula, where λ_B denotes the Bragg wavelength, which indicates the multiplication of n_{eff} – the effective refractive index and the grid period or Λ [18].

$$\lambda_B = 2n_{eff}\Lambda \quad (2)$$

It is also possible to consider a typical fiber Bragg grating characteristic (see Fig. 3 (a)), where λ_B is the center frequency or wavelength and Full Width Half Maximum (FWHM) denotes the full width of the spectrum of its reflected signal at one half of the maximum. This parameter is influenced by several parameters, in particular the width of the grid or the bandwidth of the reflected signal. Figure 3 (b) shows the spectrum of the amplitude frequency transmission curve of the reflected signal of the Bragg grating experimentally measured in the Scientific Laboratory of Fiber Optic Transmission Systems (ŠOPS) of the Communication Systems Technology Research Center of RTU Institute of Telecommunications (RTU TI SSTIC).

Nowadays, every year, the implementation of fiber optic technology is improved and expanded in the telecommunications industry, not only in business and public space but also in private sector. Of the available fiber-to-the-home (FTTH) deployment statistics, the United States, for example, to this date has reached the highest rate in the country. By 2017, the United States had increased the number of households with access to broadband fiber optic network infrastructure to 4.4 million. Overall, about 28 % of all 35 million US households now have access to fiber-optic networks [8].

Latvia is a good example of a successful implementation of the fiber optic network and maintains a leading position in the European FTTH rating with fiber coverage to the house/building, which accounted for approximately 95.6 % in September 2019 [40]. This means that in almost every home in Latvia it is physically possible to ensure the connection of a fiber optic network. Latvians are increasingly using these opportunities.

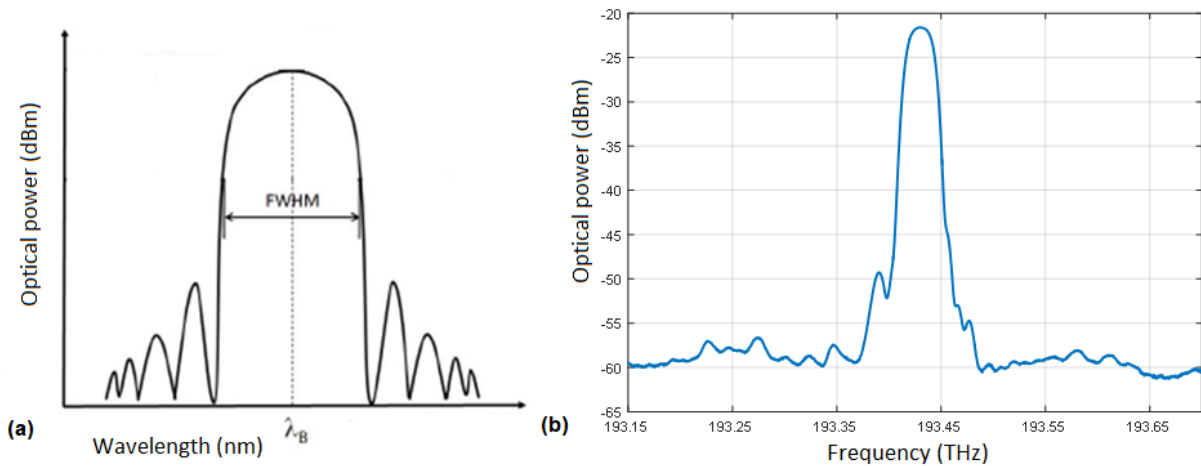


Fig. 3. Typical fiber Bragg grating reflected amplitude frequency transmission spectrum (a) and amplitude frequency transmission spectrum of Bragg grating reflected signal experimentally measured in RTU TI SSTIC ŠOPS laboratory (b) [18].

With the development of fiber optic systems and their interaction with data transmission systems, solutions have been developed to provide fast transmission over passive optical networks (PONs), which also provide an environment for fiber optic sensor deployment. The United States is working on the Connecting America: The National Broadband Plan project to provide local communities with at least a 1 Gbit/s high-speed connection. In this configuration, PON is considered to be the best solution, while providing a cost-effective way to implement the FTTH network [20].

From the standardization of broadband PON (BPON) by the International Telecommunication Union (ITU-T) G.983.1-G.983.5 in 2000 (providing a download speed of 1.25 Gbit/s and an upload speed of 0.625 Gbit/s) to the present day, when next generation Ethernet network PON (NG-PON) standardized by the ITU-T and the 802.3ca Working Group of the Institute of Electrical and Electronics Engineers (IEEE) (providing 25 Gbit/s, 50 Gbit/s and even higher data rates) is being developed and discussed. Studies related to FTTH suggest that globally, from a technological point of view, there will be a switch from 2.5 Gbit/s GPON to XGS-PON and NGPON-2 in the time interval between 2020 and 2022 [10], [20].

Until now, telecommunications networks have been divided and built into 3 main categories – long-haul networks, typically 1000 km and longer, metropolitan networks – providing a connection between a service provider and city, as well as access networks – providing a connection between the service provider and the end-user. Access networks and metro-regional networks tend to be combined into single metro-access networks, providing tens to several hundred km of connections between end-users, service providers, and regions (cities), thus opening up wider possibilities for more convenient use of different applications (e.g., optical sensors) and their governance [21].

Because of all the above, it is clear that over time, more and more users will demand access to telecommunications solutions in various locations around the world. As a result, the amount of data transferred from both users and different types of systems, such as optical sensors, will also increase. This, in turn, will necessitate the optimization of available bandwidth, increased data processing capacity, increased storage capacity, and increased data rates.

Chapter 2

The research in this chapter focuses on FBG optical sensors, with a special focus on fiber optic temperature sensors. As part of the experiment, a simulation model has been developed using RSoft software OptSim, during which the effect of temperature on the center frequencies or wavelengths of 5 FBG optical sensors have been studied. This developed optical sensor

network is combined with an optical transmission system in one common 20 km long optical fiber line. A multi-sensor network and a 50 GHz separated 4-channel non-return-to-zero (NRZ) intensity modulated, dense WDM optical communication system with a transmission rate of 10 Gbit/s per channel has been studied and evaluated (see Fig. 4).

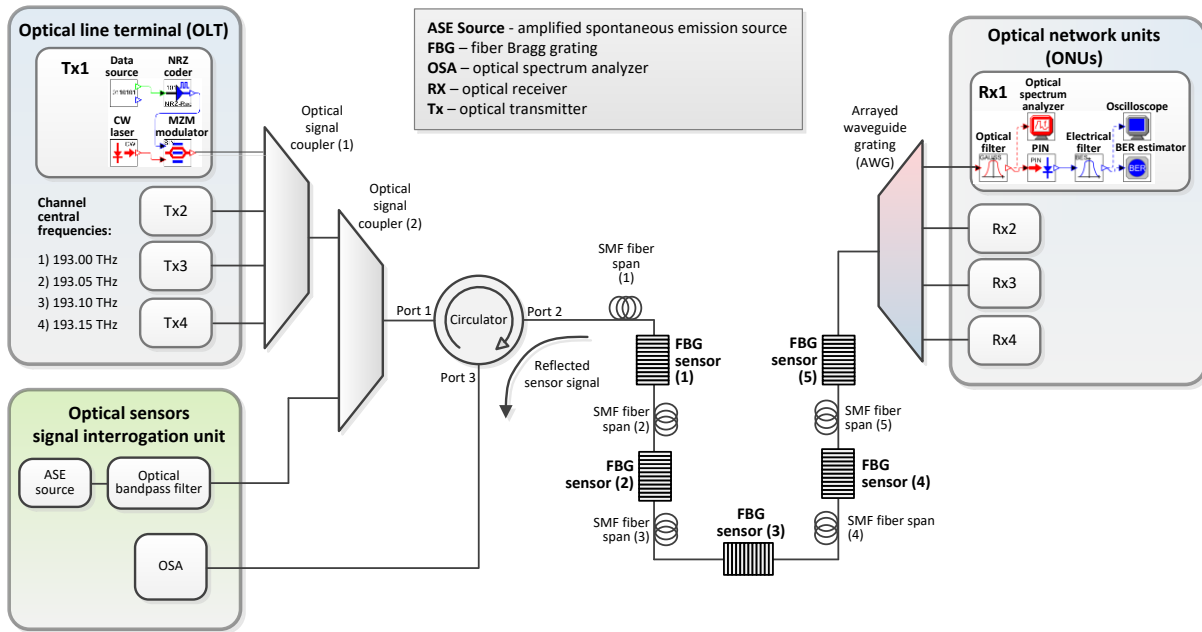


Fig. 4. Implemented system of five optical FBG temperature sensors integrated into a 4-channel 10 Gbit/s NRZ-OOK dense WDM-PON transmission system.

The most important task in the research of this chapter is the development of a flexible sensor-communication simulation model that provides simultaneous transmission of FBG optical sensors' network and data channels. It is important to study the effects of temperature changes and to understand the extent to which temperature affects the wavelengths or frequencies of the signals reflected by optical sensors. This makes it possible to determine the accuracy and practical application of these sensors. During the simulation, 5 FBG fiber optic sensors are exposed to temperature changes from $-40\text{ }^{\circ}\text{C}$ to $+120\text{ }^{\circ}\text{C}$ with an increase of $20\text{ }^{\circ}\text{C}$ (see Table I).

Table I

Temperature effect on reflected central signal frequencies of simulated FBG sensors

Temperature on the sensor ($^{\circ}\text{C}$)	Central frequency of FBG reflected signal (THz)				
	Sensor 1	Sensor 2	Sensor 3	Sensor 4	Sensor 5
-40	194,288	194,157	194,027	193,907	193,776
-20	194,268	194,137	194,009	193,889	193,758
0	194,247	194,117	193,986	193,868	193,738
+20	194,227	194,096	193,969	193,848	193,718
+40	194,207	194,076	193,948	193,827	193,699
+60	194,188	194,057	193,927	193,807	193,679
+80	194,166	194,037	193,907	193,787	193,658
+100	194,147	194,017	193,889	193,766	193,638
+120	194,127	193,997	193,868	193,748	193,618

Total temperature changes (°C)	0.161	0.160	0.159	0.159	0.158
Average calculated frequency change per 1°C (GHz)	1.0063	1.0000	1.0125	0.9938	0.9875

The data obtained from Table I show that the average calculated frequency change for 1 °C is 1 GHz, and there is a close correlation between the data obtained from all FBG sensors in this type of configuration. As the temperature increased, the frequency of the reflected optical signal by each sensor decreased, and inversely, its wavelength increased (see Fig. 5).

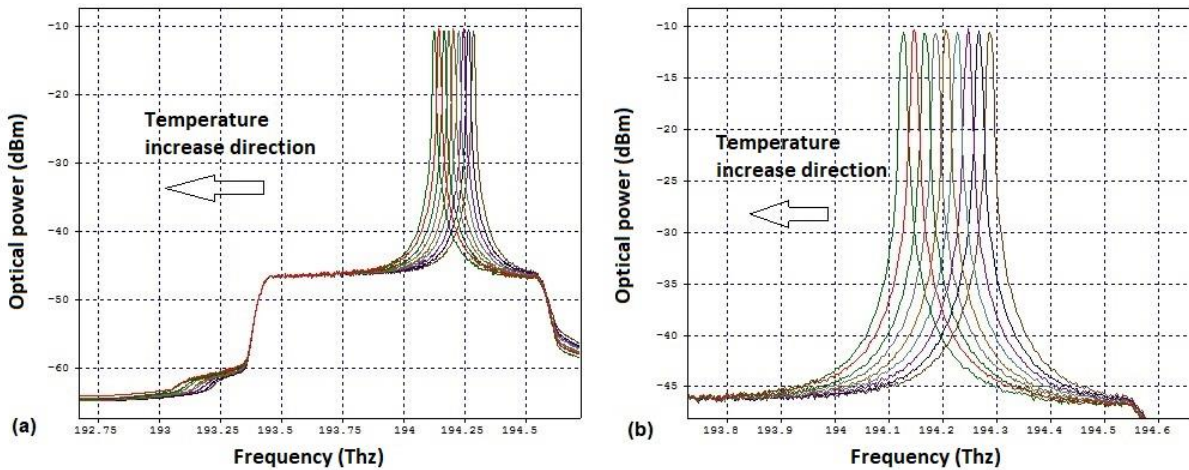


Fig. 5. First FBG fiber optical sensor's central reflected signal frequency changes due to temperature increase (a); and detailed information about first FBG fiber optical sensor's central reflected signal frequency changes due to temperature increase (b).

In Fig. 6, the received wide-open signal eye diagram shows that such an optical sensor system can be integrated into the optical data transmission system. In contrast, as can be seen in Fig. 7, using an AWG device, all four data channels can be relatively easily subtracted from the whole signal, which also includes the FBG-filtered ASE source spectrum. The author's study considers the coexistence of an FBG sensor network and a DWDM-PON 4-channel system with a transmission speed of 10 Gbit/s with a 50 GHz channel spacing on a 20 km long transmission line, ensuring error-free signal transmission (accepted BER $<10^{-9}$ [6], [17], [29]). The statistically calculated BER for the received signal is calculated as 1×10^{-40} .

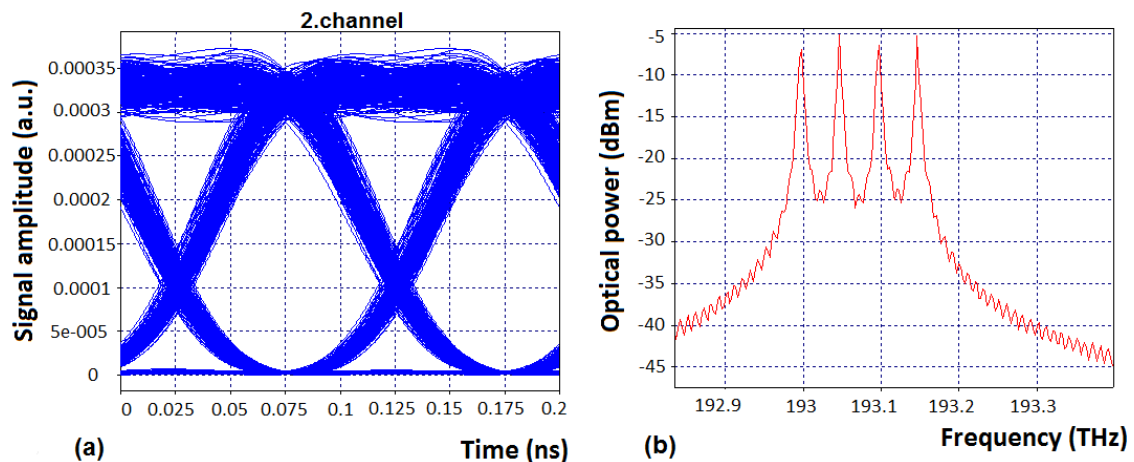


Fig. 6. (a) Eye diagram of the received signal (2nd channel) after 20 km transmission and (b) transmitted spectrum of dense 10 Gbit/s NRZ-OOK WDM transmission system with 50 GHz channel spacing.

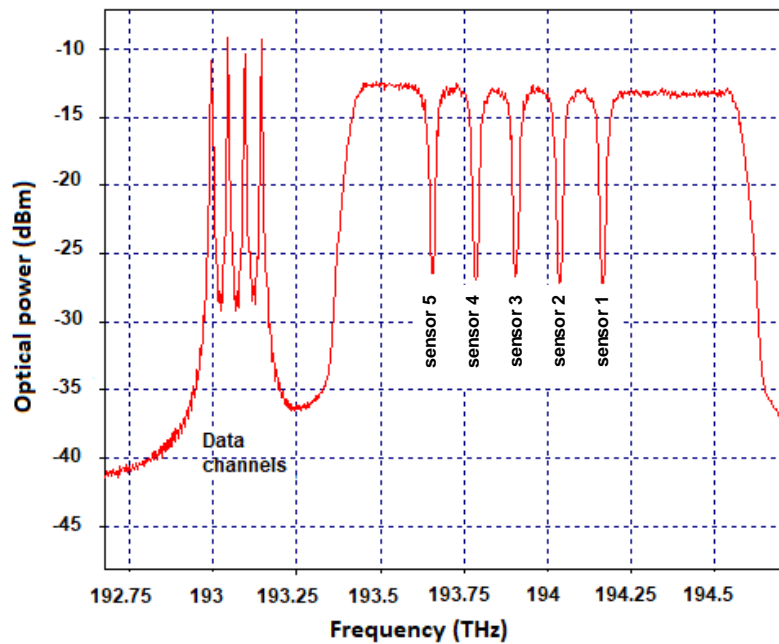


Fig. 7. Optical spectrum on the input of AWG unit, before ONUs, where four 10 Gbit/s NRZ-OOK data channels and transmission spectrum of five FBG sensors can be seen.

In general, based on the author's recommendations, such an OptSim model can be used to adjust it for further SHM object research needs.

In this chapter, one type of optical sensor technology based on the fiber Bragg grating was investigated, as well as the operation of several FBG sensors that can be placed within one optical fiber, reducing the number of signal processing equipment required for the overall system was tested. It was found that the optical network of five sensors can be fully integrated into an existing or new optical transmission system, providing error-free data transmission ($BER < 10^{-9}$) at a bit rate of 10 Gbit/s on a 20 km long, standard single-mode fiber optical line, with 4 data channels (channel spacing of 50 GHz, in accordance with ITU-T G.694.1 recommendations) [11]. Using OptSim simulation software, it has been determined that in the temperature range from $-40\text{ }^{\circ}\text{C}$ to $+120\text{ }^{\circ}\text{C}$, regardless of the default center signal frequency of the FBG optical sensor (Bragg reflected wavelength), the center frequency of the reflected signal changes on average by 1 GHz (8 pm) to $1\text{ }^{\circ}\text{C}$. The available frequency band in this configuration ranged from 192 THz to 195.9 THz, which was limited by the spectral bandwidth of the broadband ASE light source used. In view of this, it can be estimated that in the third transparency window, knowing that the expected temperature will be in the range of $-40\text{ }^{\circ}\text{C}$ to $+120\text{ }^{\circ}\text{C}$, the center frequencies of the FBG reflected signal will change by 0.16 THz or 160 GHz. Thus, at least 23 optical fiber FBG sensors can be placed on a single optical fiber. However, it is also important to remember the losses caused by each optical sensor. It should be noted that the maximum number of sensors is limited due to input losses, as well as fibers, connectors, circuits, circulators, available frequency band, and optical spectrum analyzers (used to process received sensor signals).

Chapter 3

As mentioned in previous chapters, it is important to observe and study the interaction of the FBG optical sensor network infrastructure with fiber optic data transmission systems. By studying the quality indicators of the operation of such a system, the performance of the collaborated and each system, as well as possible solutions, it would be possible to realize more efficient operation of the common system by applying joint, system-necessary, technical solutions and components. It has to be done without forgetting the efficient use and optimization

of the available optical spectrum, without compromising the quality of transmitted information and system stability.

Within the framework of this chapter, a study of the interaction of a network of 5 FBG optical sensors and a 10 Gbit/s WDM-PON fiber optic 8 data channel transmission system in a 20 km long transmission line has been developed and analyzed. An advanced precision algorithm for processing the spectral peaks of the FBG sensors' reflected signals has been developed. Within the framework of this co-operation system model, a mathematical equation has been developed, which determines the minimum allowable optical channel spacing (~208 GHz). Further in this chapter, the development of a hybrid 10 Gbit/s WDM 8 data channel communication system, 2.5 Gbit/s 7 hidden data channels, and a 5 optical sensor network in a 20 km long transmission line, which is useful for steganography, is discussed. An evaluation of the visualization of the spectral characteristics obtained by this developed model has been performed and performance analysis made.

RSoft OptSim software was used to create the simulation, which used the measured amplitude frequency response data obtained from a commercially available optical temperature sensor. The existing optical sensor is a sensitive, durable temperature sensor based on FBG technology. This modeling aims to develop a simulation operation model that provides a successful interaction of the FBG optical temperature sensor network and dense 8 channel wavelength division multiplexed passive optical network (DWDM-PON) (see Fig. 8).

The developed model was further used to monitor the effect of temperature on sensor signals (optically reflected signals from FBG) as well as to observe and calculate the minimum channel spacing, which was essential for the further analyzed and developed algorithm for determining the center frequency peaks of optical sensors' reflected signals. As for the data transmission in the developed system, this model uses the NRZ-OOK non-return-to-zero on/off keying modulation scheme. OLT with 10 Gbit/s transmitters is on the service provider's side.

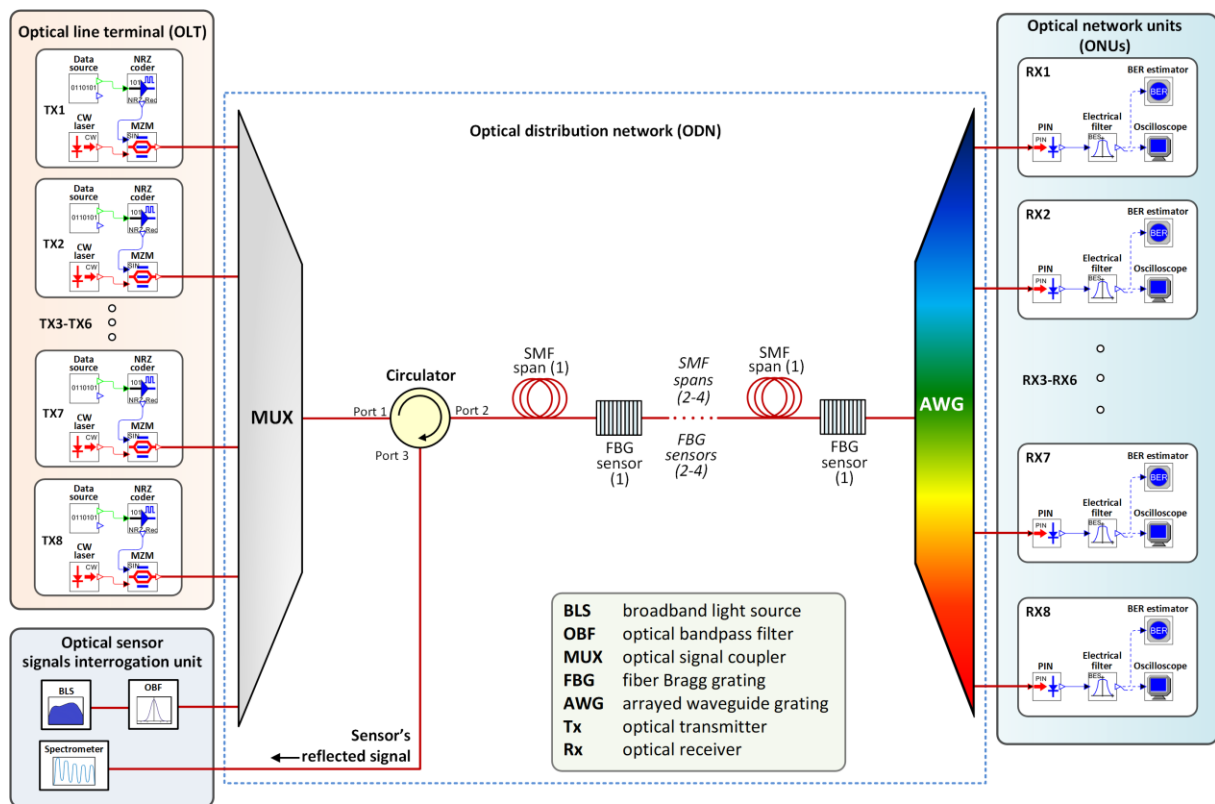


Fig. 8. Developed system model, which includes a network of 5 FBG temperature sensors and is combined with an 8-channel 10 Gbit/s NRZ-OOK DWDM-PON transmission system.

In the implementation of this study, accurate determination of the minimum channel spacing for optical sensors, as well as determination of the central frequency maximum of reflected signals using various methods, is essential. According to the technical specification of a commercial optical FBG temperature sensor, its calibrated frequency at +26 °C is 191.53713 THz or 1565.191 nm, but the frequency response to temperature changes is 1.279 GHz for 1 °C. The reflectivity of this FBG temperature optical sensor is greater than 15 %.

Figure 9 shows the simulated spectrum of the combined system at 0 °C ambient temperature, which includes 5 optical FBG sensor channels (FBG reflected signals) as well as 8 data channels that are measured with a spectrometer that is embedded in the simulation model (bandwidth resolution set to 0.07 nm and inserted inside the optical sensor signal interrogation unit). It is important to emphasize that the spectrum of the frequency response curve of this amplitude is the spectrum of the reflected signal and not the spectrum of the transmitted signal, thus, 8 data channels are shown here as significantly attenuated.

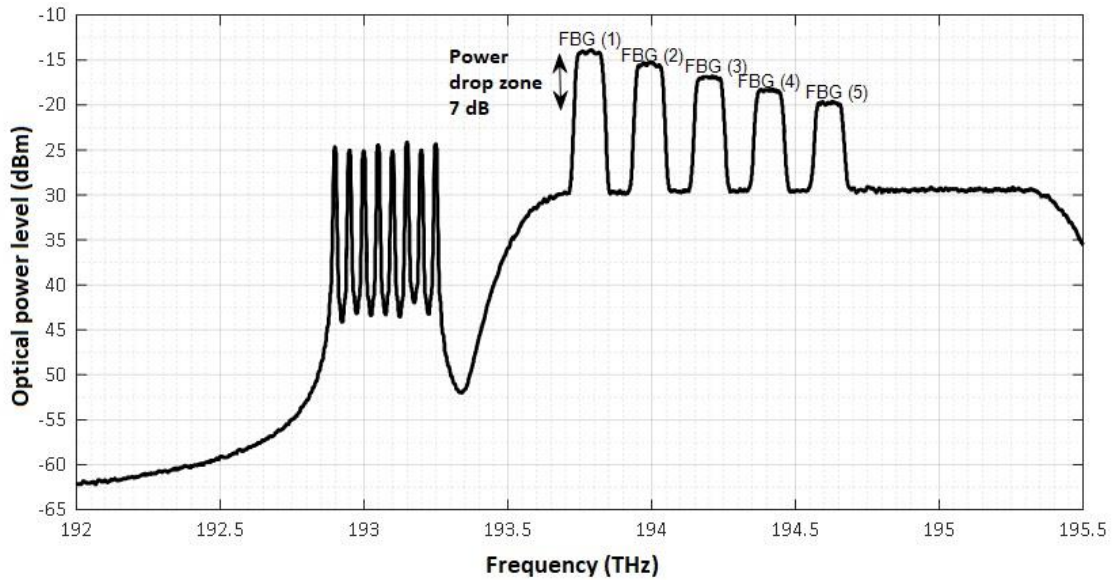


Fig. 9. The spectrum of simulated combined system with 5 FBG optical sensor reflected peaks and 8 data channels (spectrum obtained by spectrometer located in optical sensor interrogation unit) at 0 °C environment temperature.

The operating temperature of the FBG sensor, depending on the configuration, is expected to be in the range of 80 °C (–20 °C to +60 °C), typically as seen in SHM applications. Knowing the frequency, which is the temperature response, as well as the spectral width of the central frequency peaks of the FBG optical sensors' reflected signals, an equation has been developed to determine the theoretically minimum channel spacing (CS) between each optical sensor integrated into the existing system.

$$CS = bw_{avg} + (T_{tot} \cdot f_{var}), \quad (3)$$

where CS (GHz) is the sensor's channel spacing, bw_{avg} (GHz) is the average spectral width of the signals reflected by the FBG sensors in the optical power drop zone of 7 dB, T_{tot} (°C) is the sum of the intended or expected temperature fluctuations, and f_{var} (GHz) is the response of the FBG temperature sensors' reflected signal changes in their central frequency, in other words, a change in frequency to 1 °C. The experimental measurement of this value was reported earlier in this chapter. After inserting all known variables into the equation, the calculation of the sensor's minimum channel spacing is shown further:

$$CS = bw_{avg} + (T_{tot} \cdot f_{var})$$

$$= 109.8278 + (80 \cdot 1.231) = 208.285 \text{ GHz} . \quad (4)$$

The author offers an accurate solution for determining the center frequency peaks of the reflected signals of optical sensors, which has been developed within MATLAB software. The working structure and the sequence of sensor signal processing are visualized in the diagram (see Fig. 10). Figure 10 illustrates the research process from the simulation model to the development of an algorithm (Matlab algorithm) to determine the exact center frequencies of the optical sensors' reflected signals.

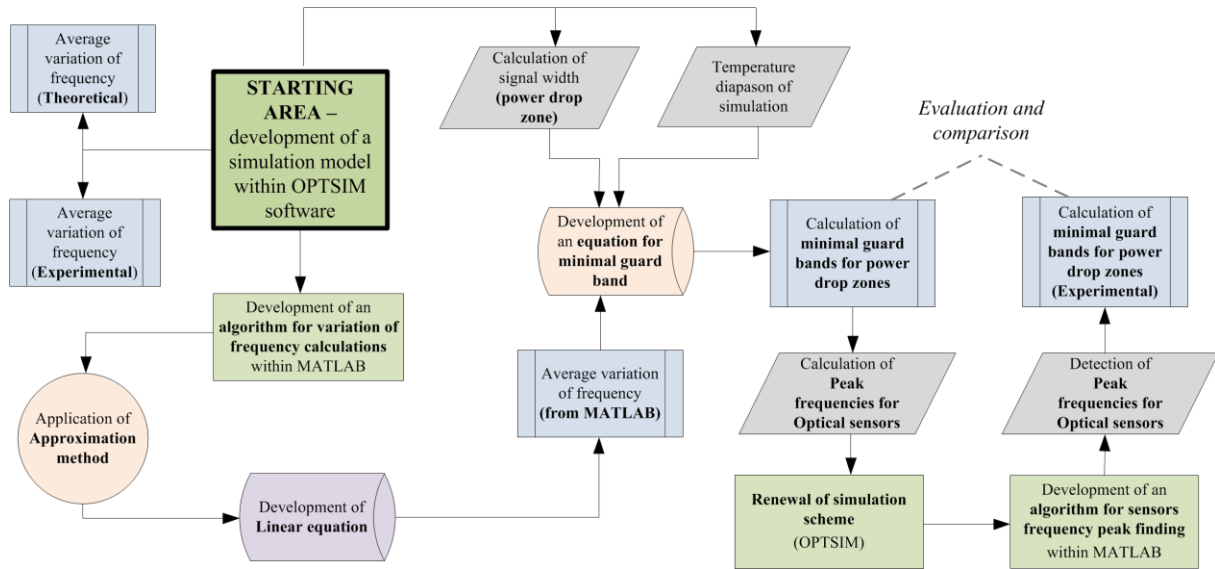


Fig. 10. Flowchart of the algorithm development for precise detection of the exact center of the signal's peak (central frequency).

To be sure that the exact spacing between the channels of the optical sensors is determined, it is important to find the exact maximum of the center of each signal and vice versa. It should be clarified that the highest value in the peak region of the reflected signal of the optical sensor is not always its center. In this situation, all kinds of standard algorithms used (shown as "x" in Fig. 11), which provide an automatic search for peaks of reflected signals of optical sensors, unlike the algorithm proposed by the author, do not provide the required results, as shown in Fig. 11.

Knowing that the FBG channel spacing is calculated as the difference between two adjacent FBG signal peak centers and that the newly acquired maximum center frequency values will change during the calculation, it was understood that the channel spacing or distance will also change. Therefore, Table II summarizes the determined new center frequencies for the FBG optical sensor signal peaks as well as a comparison with the previously obtained values, which were calculated according to the initial, standard optical spectrum peak reading method. These results can also be used to determine and compare channel spacing values.

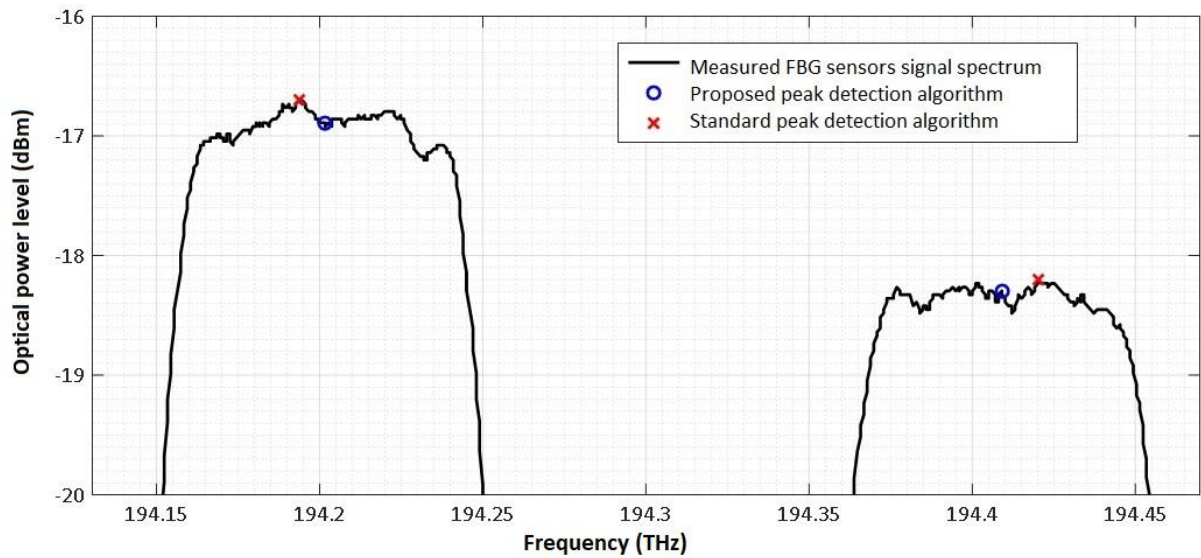


Fig. 11. Comparison between standard automatic peak detection algorithm, based on the highest value in the peak region, and proposed algorithm, which detects the exact center of the peak for FBG Sensors 3 and 4.

As shown in Table II, there is a difference (GHz) between the calculated and measured frequency values. This value represents the difference in error between the two algorithms used.

Table II

Calculated and detected FBG optical sensor central signal frequencies using both methods

FBG sensor's no.	Central peak frequency (THz) obtained by		Difference (GHz)
	Calculated central frequencies	Measured with a proposed peak detection algorithm	
1	193.800	193.785	15.166
2	194.008	193.994	14.084
3	194.217	194.201	15.385
4	194.425	194.409	15.642
5	194.633	194.616	17.322
Channel spacing (GHz)	208.285	207.746	0.539

From the obtained results, it is clear that such a peak detection algorithm can be integrated into the FBG optical sensor interrogation unit to perform an even more accurate determination of the central peak of the reflected signal of each FBG optical sensor and application of the channel spacing values.

This chapter shows a 5 FBG optical sensor network and an 8-channel NRZ-OOK modulated 10 Gbit/s optical fiber data transmission system. During the study, an equation is developed to calculate the minimum channel spacing of optical sensors, which allows determining a certain minimum frequency band between adjacent optical FBG sensors, ensuring that their reflected signals do not overlap in the specified frequency range. The obtained results showed that in this configuration, the channel spacing between the adjacent FBG temperature sensors must be provided of at least 208 GHz. Traditionally used algorithms for estimating the frequency peaks of the optical sensors' reflected signals determine that this central frequency is the point of the peak with the highest intensity – value. However, the

highest point is not always the exact center of the frequency peak of the optical sensor, given the power fluctuations and the irregularity of the FBG reflected signal's frequency spectrum. In this chapter, therefore, an algorithm for determining the exact center frequencies of such signal peaks is proposed and validated. The algorithm has a direct application in FBG signal processing solutions.

In this chapter, a hybrid WDM communication system with stealth data channels and fiber optic sensor networks is also developed. In previous studies [15], [28], WDM data channels are combined with ASE noise (representing stealth data transmission or channel masking in the directly available ASE spectrum). In this work, instead of reserving the entire frequency spectrum occupied by the ASE, which is reserved for stealth data in the frequency band, the author's study is performed differently. A single, modulated ASE slice containing hidden data is inserted between each WDM-PON data transmission channel that is based on the laser light source, as shown in Fig. 12.

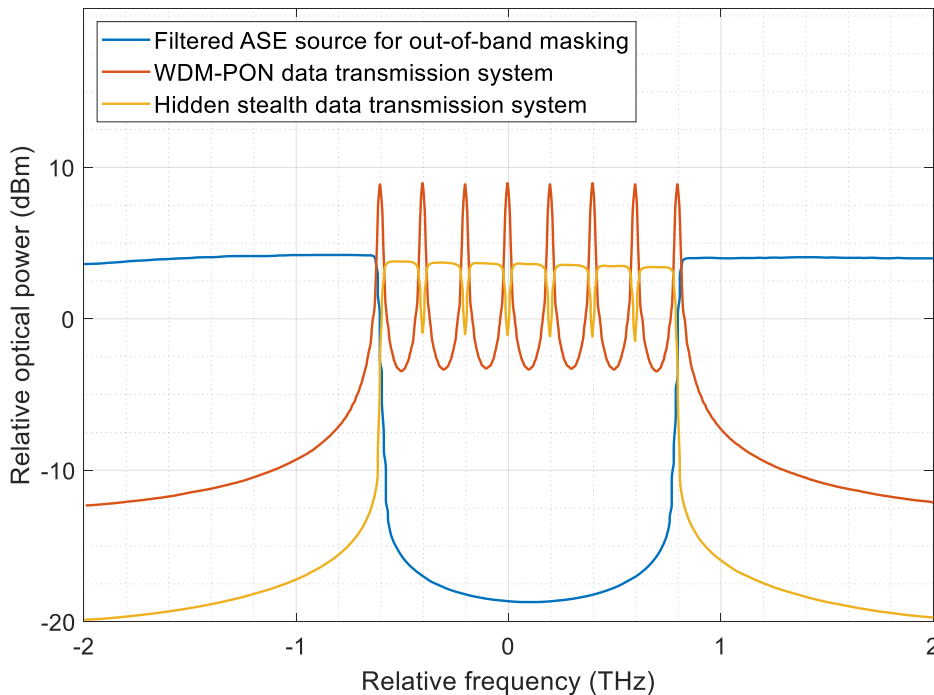


Fig. 12. Proposed spectrum allocation of the laser-based WDM-PON and spectrum-sliced ASE-based stealth transmission system (optical spectrum measured before launching signal into 20 km long transmission fiber span).

Another source of ASE is used to add ASE noise outside the hybrid WDM-PON and stealth channel system frequency band, which is required to perform spectrum smoothing and is available to other frequency spectrum users and their needs [26], such as, for instance, for optical sensor network, as it is done in this study. As mentioned in several publications [5], [23], limiting the ability to observe and analyze the regularities of transmitted data is critical to provide a valuable additional layer of security in optical communication networks that additionally complements data encryption mechanisms.

The developed simulation scheme includes a typical WDM-PON system architecture (except for the stealth data transmission system) and is shown in Fig. 13. In general, this hybrid fiber optic communication system consists of CO, ODN, and ONT. The central office has two main types of OLT consisting of different transmitter blocks – one for the WDM-PON system (OLT1) and the other for the ASE source-operated, stealth channel system (OLT2). In addition, another ASE source (ASE1) together with a transient, notch optical filter is used in the central office to provide stealth channel masking outside the optical, stealth channel system's, operating range. This light source will also be the basis for the operation of optical sensors, thus

also optimizing the use of existing resources. Like the transmitter part, the receiver part has two types of receivers – one for receiving and processing WDM-PON data transmission channels and the other for receiving spectrally sliced ASE stealth data channels.

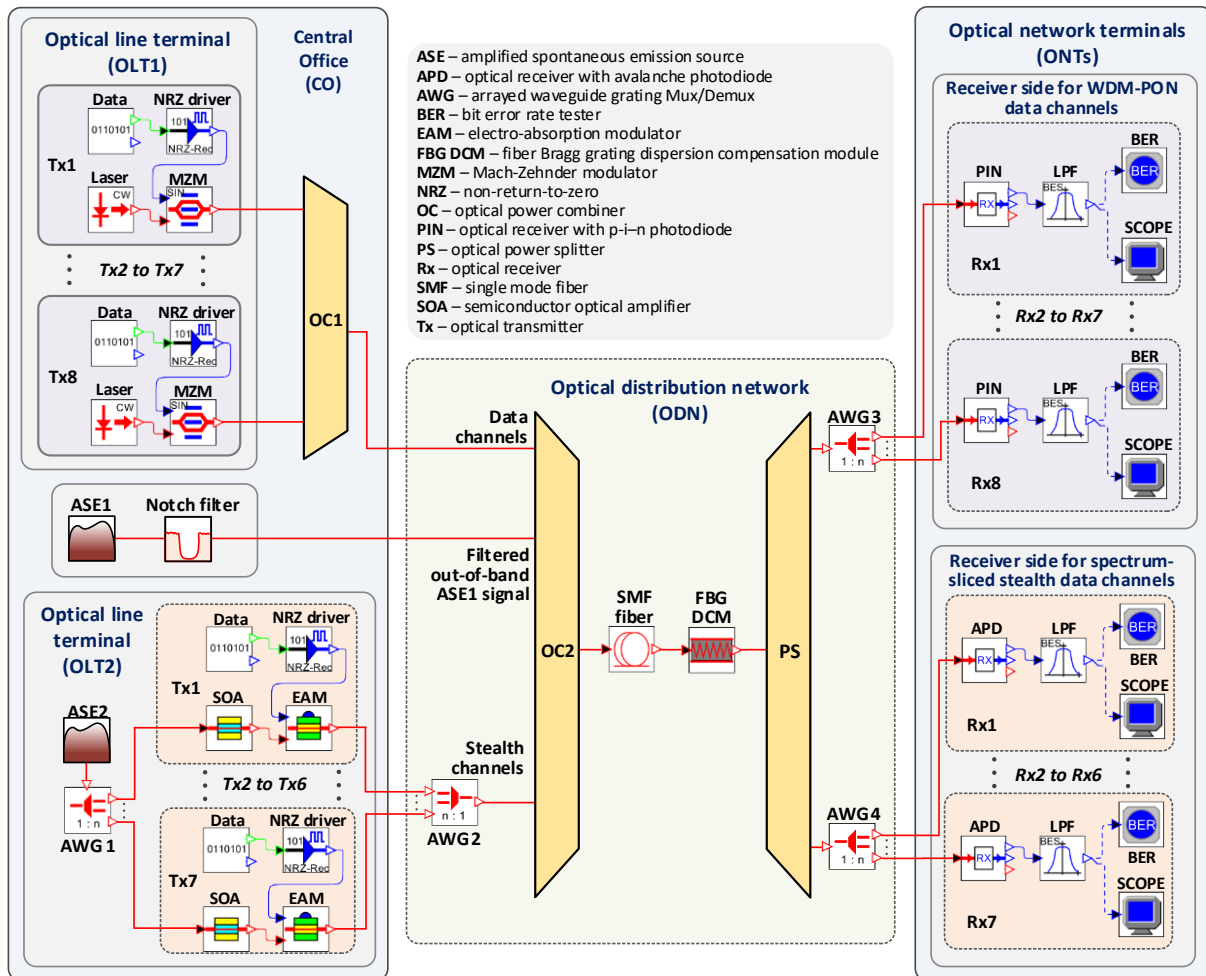


Fig. 13. Simulation of a hybrid fiber optical communication system containing 8-channel 10 Gbit/s (10.7 Gbit/s including 7 % FEC OH) NRZ-OOK modulated WDM PON transmission system part (upper part) and 7-channel 2.5 Gbit/s (2.675 Gbit/s including 7 % FEC OH) NRZ-OOK stealth channel system part (lower part).

Taking into account the 7 % data overhead (FEC OH), the simulated bit transmission was 10.7 Gbit/s. A CW laser with an output power of +3 dBm and a 3-dB line width of 50 MHz was introduced as a light source for OLT1. The captured spectrum of the OLT1 output amplitude frequency transmission curve is shown in Fig. 14 (a).

In the middle of the left part of the CO there is the first ASE 1 light source, which was important to evenly set the signal power level in the total spectrum (outside the operating range of WDM-PON 8 data channels), thus helping to smooth the masking of stealth data channels. The filtered ASE 1 signal is then transmitted to the optical combiner (see Fig. 14 (b)). Finally, on the lower left side of the CO there is OLT 2 with 7 stealth signal transmitters (Tx1 to Tx7). The determined transmission spectrum of the OLT 2 output optical amplitude frequency response is shown in Fig. 15 (a).

The proposed hybrid system has tested two transmission scenarios – B2B and with a 20 km long single-mode fiber optic transmission line. The captured optical amplitude frequency response spectrum containing all three signals (data channels, first filtered ASE used for masking stealth data channels, and ASE stealth data channels) after a 20 km long single-mode fiber transmission line is shown in Fig. 15 (b).

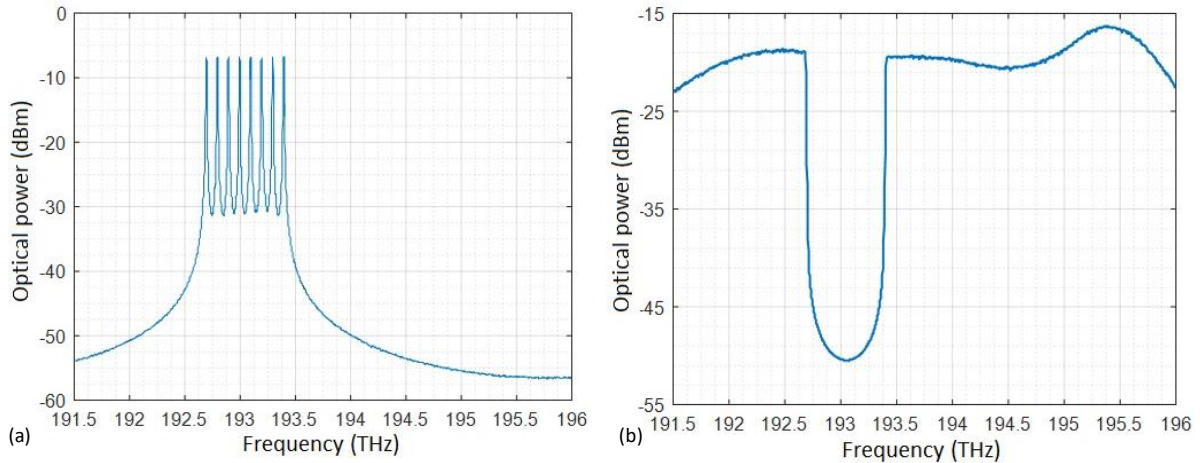


Fig. 14. (a) – Simulated amplitude frequency response spectrum for an 8-channel WDM-PON transmission system (10.7 Gbit/s transmission rate); (b) –ASE 1 source filtered with a broadband (710 GHz 3-dB bandwidth) type filter to mask spectrally sliced data channels.

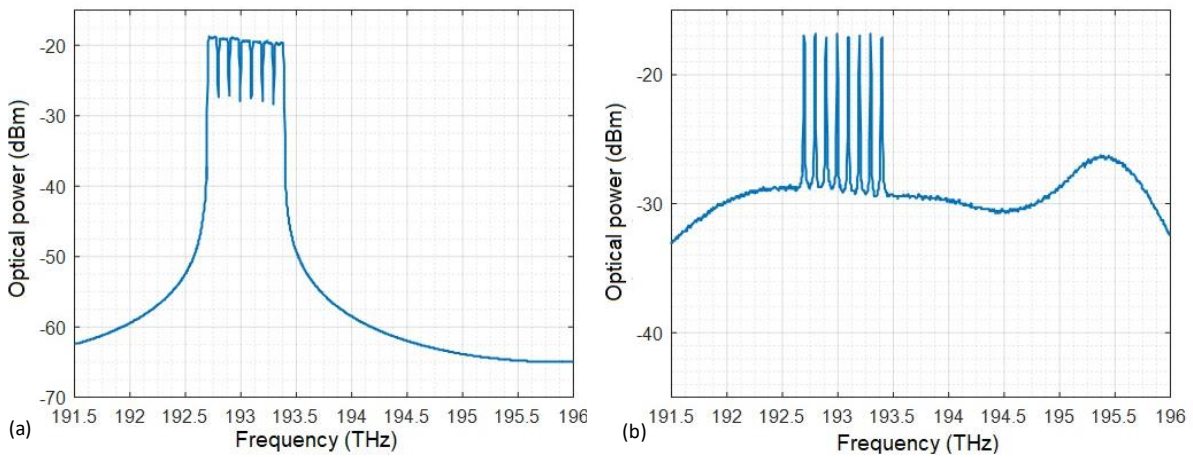


Fig. 15. (a) – AWG2 output amplitude frequency response curve of spectrally sliced 7 stealth data transmission channel system (2.675 Gbit/s bit rate) spectrum; (b) – the received optical amplitude frequency response spectrum (data channels, filtered ASE used to mask ASE stealth channels and ASE stealth channels) of all three signals after a 20 km transmission line.

Finally, it is particularly important to compare BER versus received optical power of all scenarios to understand the amount of signal distortion that a stealth system can introduce into a WDM-PON system (see Fig. 16). Figure 16 shows a direct correlation between all scenarios, so it is safe to say that the insertion of stealth data channels is effectively possible in such system collaboration models.

Numerically, referring to Fig. 16, it is necessary to perform a power penalty calculation for a WDM-PON system with and without the inclusion of a stealth channel system in the overall transmission system architecture. Table III shows that in the B2B as well as the 20 km transmission line configuration scenario, the power penalty between the two (simple WDM-PON system versus WDM-PON system with stealth data channels) is less than 0.5 dB.

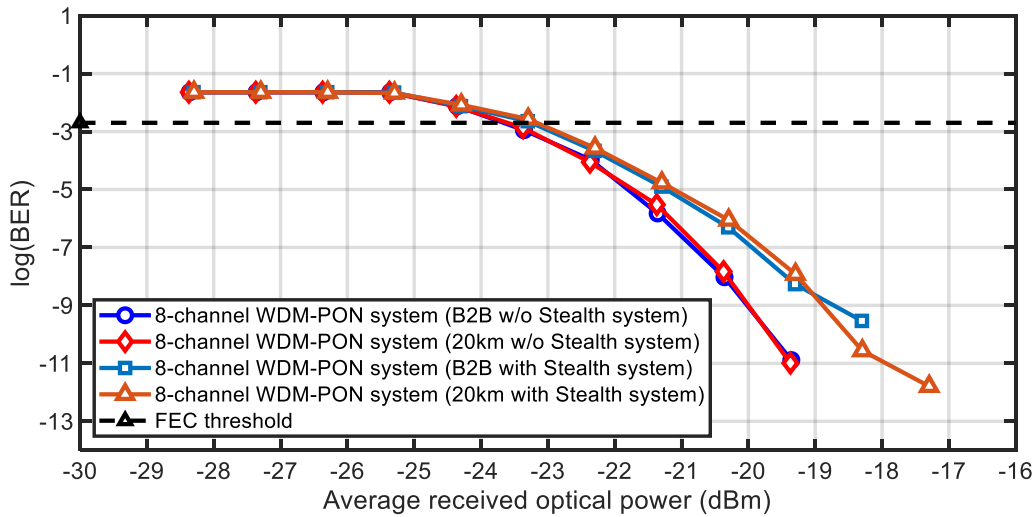


Fig. 16. BER versus received optical power for 8-channel WDM-PON data transmission system in B2B condition versus 20 km long transmission line with and without stealth system integration.

From Fig. 16 and Table III, it is possible to observe important factors related to the integration of stealth signals in WDM-PON data transmission systems. First, there is a strong correlation in the BER results between the B2B transmission scenario and the 20 km transmission. This means that the proposed model of a combined hybrid system does not negatively affect the performance of transmission distances typical of optical access networks, such as 20 km. Second, the integration of the spectrally sliced stealth system still provides a sufficiently high quality of WDM-PON data transmission – the calculated power penalty is insignificant in all conditions at the pre-FEC BER level of 2×10^{-3} (according to ITU-T G.975.1 standard and accepted practice in scientific publications [12], [14], [30]).

Table III

Power penalty between a simple WDM-PON system and a WDM-PON system with a spectrally sliced stealth system proposed by the author

Simulated scenario	Power penalty at the pre-FEC BER level of 2.3×10^{-3}
10.7 Gbit/s WDM data channel system at B2B configuration (with Stealth system)	0.42 dB
10.7 Gbit/s WDM data channel system at B2B configuration (without Stealth system)	
10.7 Gbit/s WDM data channel system at 20 km long transmission line configuration (with Stealth system)	0.43 dB
10.7 Gbit/s WDM data channel system at 20 km long transmission line configuration (without Stealth system)	

Taking into account the solution implemented and the successful integration of stealth data channels in the WDM-PON system, the integration of 5 FBG optical sensors' network in the collaborated system is further integrated and monitored. Figure 17 shows the new scheme supplemented by the upper middle part. There are 5 FBG optical sensors in the optical transmission line, between the transmitting and receiving sides. Each of these sensors is

separated by a 4 km long SMF fiber span. The channel spacing of the optical sensors, as discussed in previously, is set to 208 GHz width between each optical sensor signal.

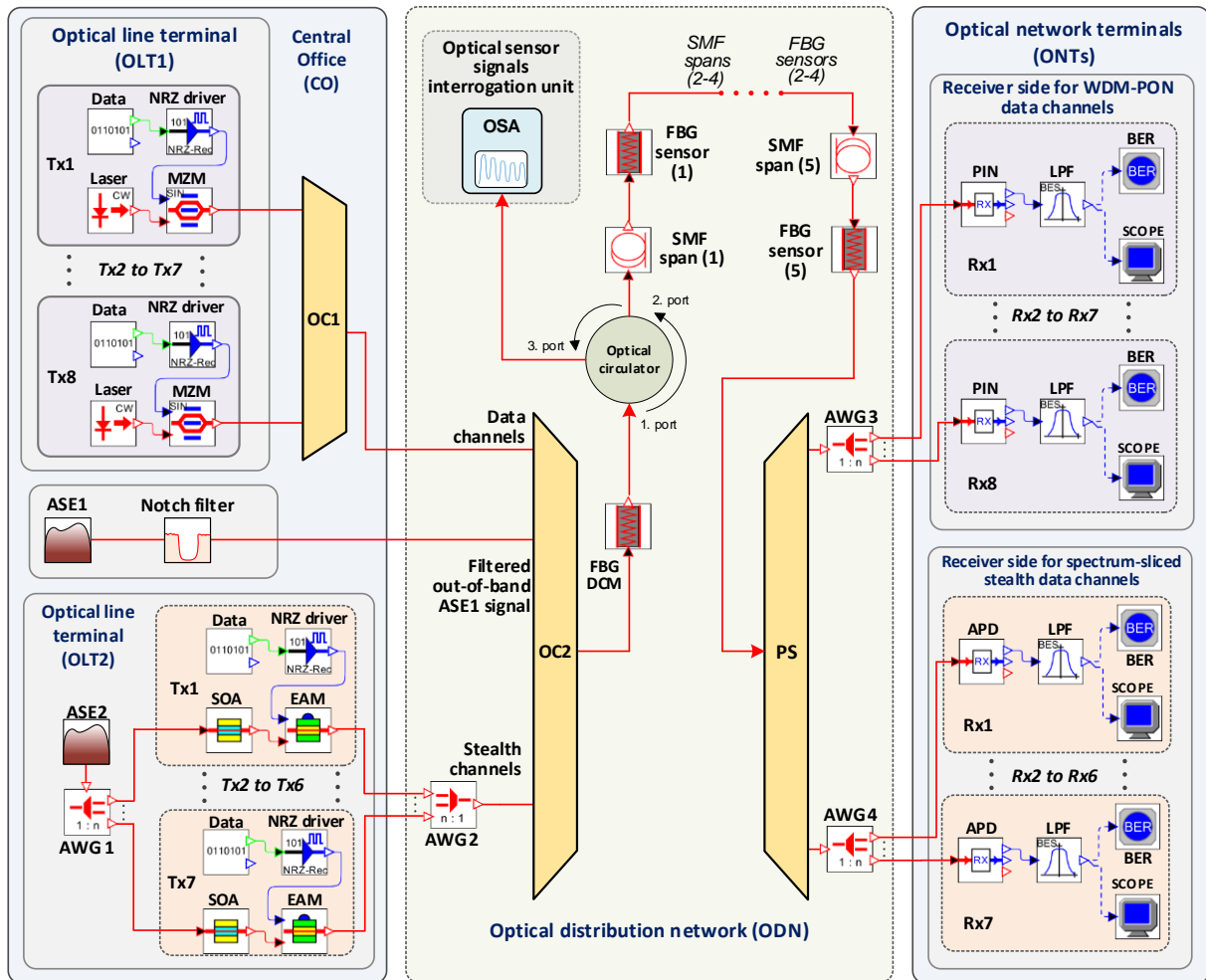


Fig. 17. Hybrid optical communication system simulation scheme with 8 data channels, 7 hidden data channels, and 5 FBG optical sensor systems.

Figure 18, on the other hand, shows the spectrum of the amplitude-frequency transmission characteristic of the reflected signal, which can be observed in the optical sensor interrogation unit using the optical spectrum analyzer. It is important to note here that the reflected signal in the collaborated system is transmitted in double amount. This means that after the entire length of the optical transmission line, the optical signal is reflected – retransmitted through the entire collaborated system through each optical sensor which is separated by a distance of 4 km from each other. It also affects the difference between the peaks of the signal reflected by the optical sensors and the overall spectrum.

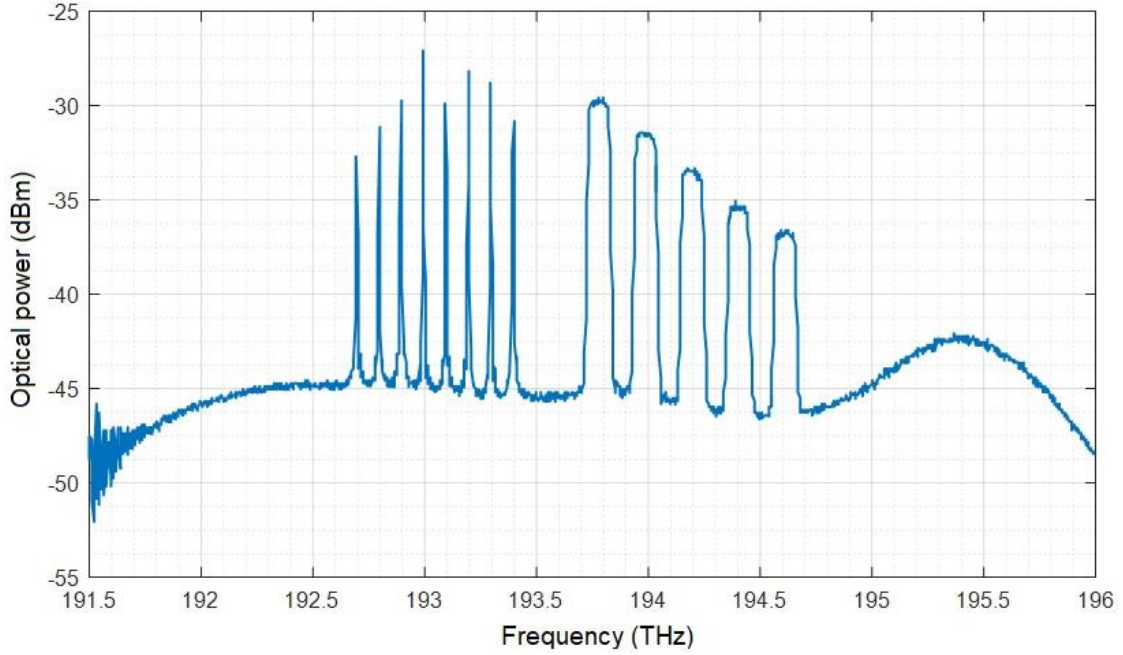


Fig. 18. Optical amplitude frequency transmission characteristic spectrum of the reflected signal of a hybrid optical communication system.

Next, using the predefined system element configuration to ensure that the hybrid system configuration does not adversely affect the WDM-PON data channel and stealth data channel systems, the received signal quality is considered by analyzing the eye diagrams (as shown in Fig. 19).

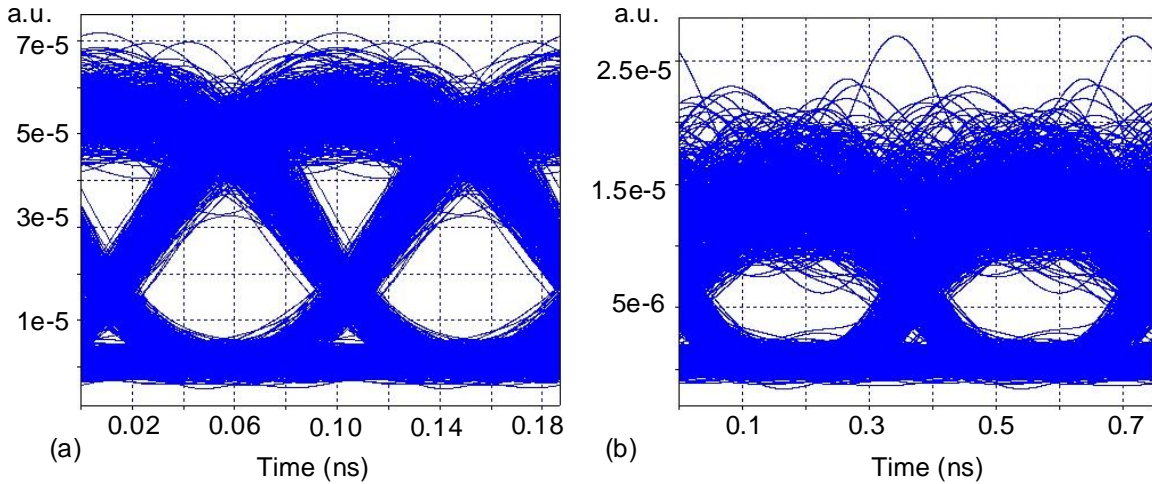


Fig. 19. (a) – Eye diagram for the worst-performing WDM-PON data transmission channel (2nd channel); (b) – eye diagram for the worst-performing stealth data channel (5th channel) in a 20 km long transmission line.

During this scenario, in the implementation of the hybrid configuration with data channels, stealth data channels, and optical sensors, the highest BER of the stealth data channels was observed for channel 4, which is 2.16×10^{-5} . For data channels, it is channel 2 with a BER value of 2.86×10^{-16} . The average BER of the stealth data channels is 1.11×10^{-5} , while the average BER of the WDM data channels is 7.16×10^{-17} . Table IV compares the BER averages for WDM-PON data and stealth data channels with and without optical sensor system integration to better understand the effect of the optical sensor system on stealth data channel and WDM-PON data channel quality.

BER averages for WDM-PON data channels and stealth data channels with and without optical sensor system integration after a 20 km transmission line

Average BER value	Without optical sensor system integration	With optical sensor system integration
WDM-PON data channel system	7.23×10^{-19}	7.16×10^{-17}
Stealth data channel system	1.13×10^{-6}	1.11×10^{-5}

As shown in Table IV, the average BER values obtained show that the insertion of the 5 FBG fiber optic sensor system did not have a significant negative impact on the WDM-PON and stealth data channel systems and the quality of their received signals. This means that such a hybrid solution can be implemented and improved for future needs.

Chapter 4

Firstly, the simulation has been successfully implemented in the study of this chapter, which combines a 7 FBG sensor system with a spectrally sliced 32-channel wavelength division multiplexed passive optical network (SS-WDM PON) data transmission system. The length of the standard single-mode fiber spans between each optical sensor in this 7 optical sensor system is 4 km. The operation of this system on a 28 km long transmission line is shown. The author offers a spectrally efficient solution in the optical part of the developed system, combining input light sources – using a single BLS between the two combined systems, rather than using a different light source for each of them. Mathematical modeling and simulation software was used to do this and to develop a unified system model, its characteristics, and performance evaluation. Performance evaluation was done in 4 different scenarios – with and without cooperation between the two systems (data channel and optical sensor) and with a bit rate of 2.5 Gbit/s and 10 Gbit/s for each data channel, confirming that realization of data transmission and optical sensor systems combination, using a single light source, is possible. In turn, later in this chapter, the development of an experimental model will be presented, where a spectrally sliced WDM transmission system with an integrated FBG optical sensor system operates on a single broadband light source. To more efficiently analyze the operation of the experimental scheme, an additional simulation scheme will be developed and adapted according to the configuration of the experimental scheme to better compare the accuracy of the obtained data. Such a set of schemes will allow to analyze the implementation of system interoperability using a common broadband light source.

Such simulations have been developed using RSOF mathematical simulation software OptSim. To prove the successful interaction of both systems – optical fiber sensor and data transmission channel, the author has developed two simulation models (see Fig. 20).

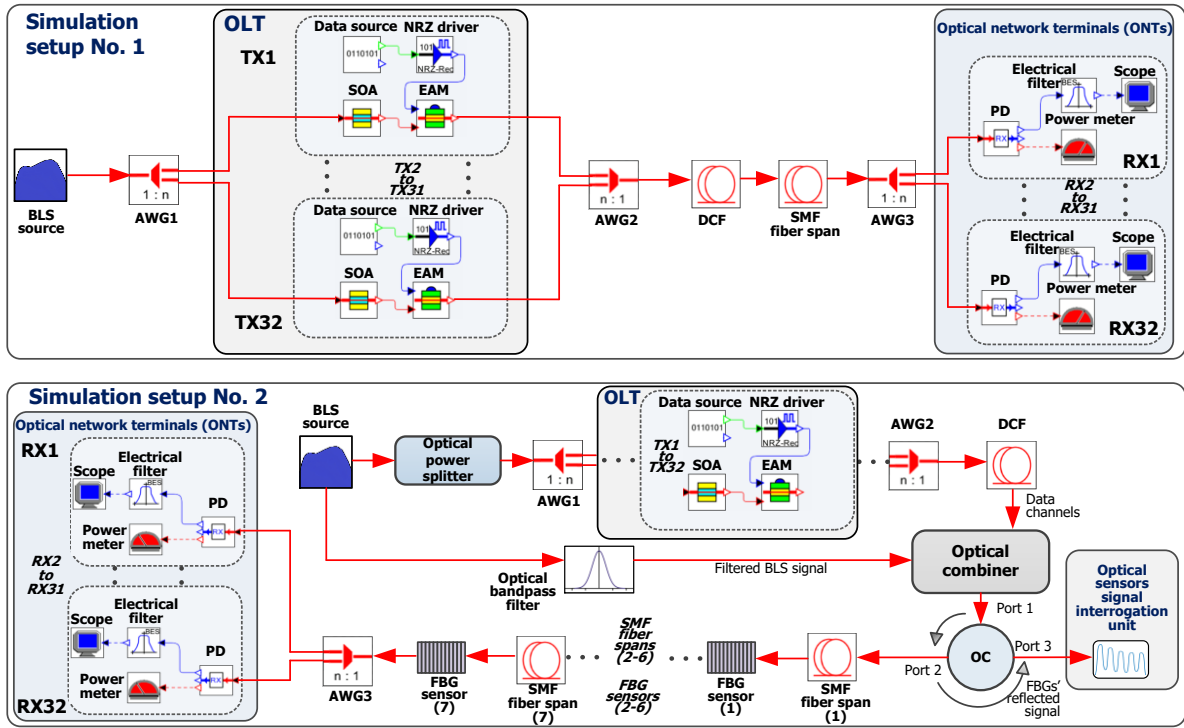


Fig. 20. Simulation models for both setups, where one shared optical fiber and optical light source are used for 32-channel SS-WDM PON transmission system (operating at 2.5 Gbit/s and 10 Gbit/s bitrates) with and without an embedded 7 fiber optical FBG sensors system (BLS – broadband light source, AWG – arrayed waveguide grating, OLT – optical line terminal, TX – optical transmitter, SOA – semiconductor optical amplifier, EAM – electro-absorption modulator, DCF – dispersion compensation fiber, FBG – fiber Bragg grating, OC – optical circulator, RX – optical receiver, SMF – single mode fiber, PD – photodiode).

The SS-WDM PON system has been successfully implemented and includes a combined system, where one is a system of 32 data transmission channels and the other is a system of 7 FBG optical sensors (with set central signal peak frequencies 193.6 THz, 193.8 THz, 194.0 THz, 194.2 THz, 194.4 THz, 194.6 THz and 194.8 THz). Both systems share one common transmission environment – an optical line and one BLS light source. Secondly, it is possible to quantify and visually determine the impact on the data transmission system in a simulation when an optical sensor system is embedded in a common scheme. This evaluation is performed at two different bit rates to see the impact on the data transmission system. The reflected spectrum of the optical signal amplitude frequency transmission curve with a 32-channel SS-WDM PON transmission system (with 2.5 Gbit/s bit rate) and a built-in 7 FBG optical sensor network is shown in Fig. 21.

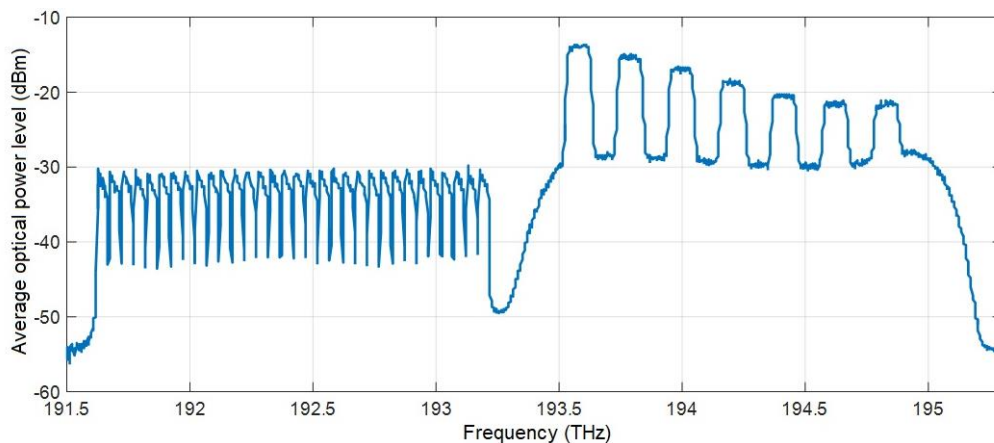


Fig. 21. The reflected optical signal spectrum of simulated 32-channel SS-WDM PON transmission system (operating at 2.5 Gbit/s bitrate) with embedded 7 FBG sensors network.

Figure 22 shows the BER in relation to the received optical power for a 32-channel 2.5 Gbit/s SS-WDM PON system with and without an integrated FBG optical sensor network. As can be seen, first, there is a close correlation between the two simulation architectures and the parameters of their optical components. This means that, in general, the insertion of the FBG optical sensor system does not adversely affect the SS-WDM PON data transmission system at a bit rate of 2.5 Gbit/s.

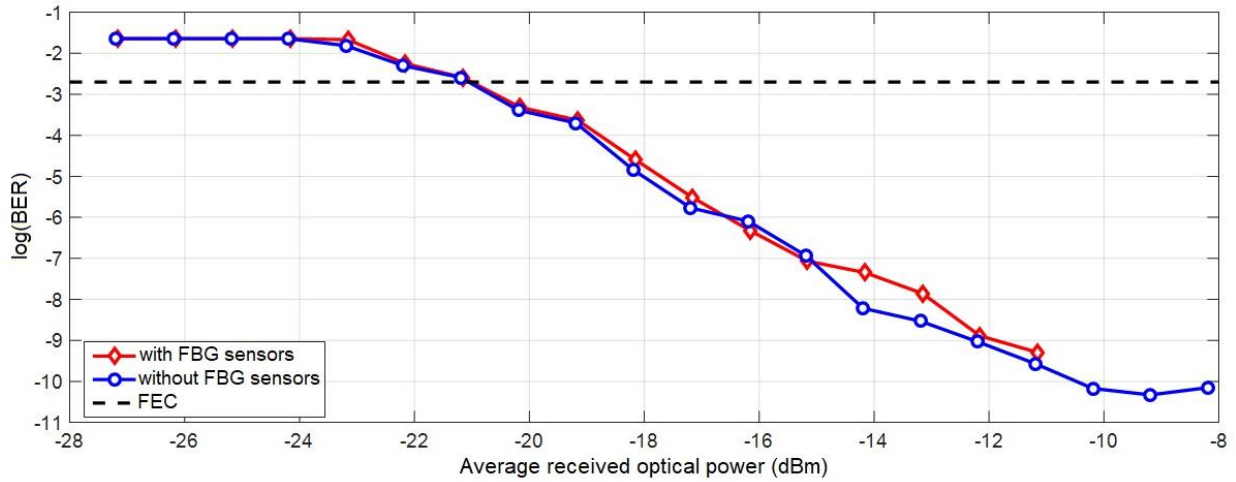


Fig. 22. BER versus received optical power for 32-channel 2.5 Gbit/s SS-WDM PON system with and without integrated FBG optical sensor network.

If measurements are made for both simulation settings at the same average received optical power, only a small BER difference can be observed for the channel. Second, the calculations show that the power penalty for the second simulation version (with optical sensor system integration) is 0.1 dB at the pre-FEC BER level of 2×10^{-3} when compared with the first simulation model result data (see Fig. 20).

Figure 23 shows a comparison between BER and received optical power for a 32-channel 10 Gbit/s SS-WDM PON system with and without an integrated FBG optical sensor system for one of the data transmission channels. Although there is a slight difference between a system with and without an integrated FBG optical sensor network at some of the received optical power points (this may be due to some insignificant measurement errors), still a strong correlation between the two simulation models and their results can be observed.

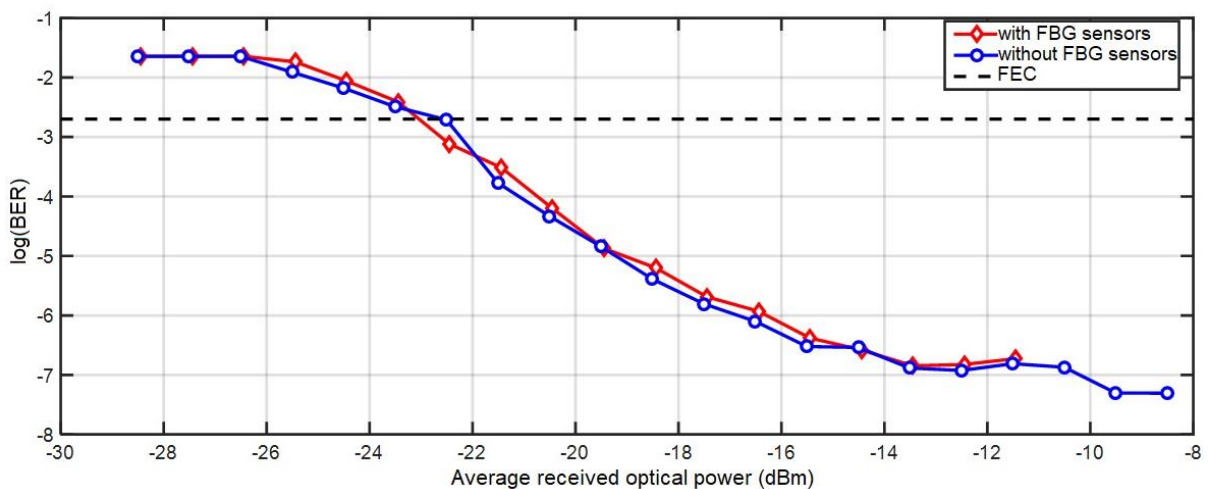


Fig. 23. BER versus received optical power for 32-channel 10 Gbit/s SS-WDM PON system with and without integrated FBG optical sensor network.

These results also show that even an increase in the bit rate (10 Gbit/s in this scenario) for a given system does not negatively affect the BER of the received signal. The only disadvantage of such a model is that it becomes more complex – additional optical, electro-optical, and electrical components and equipment are required, thus the losses brought into the overall system may increase.

Within this chapter, the author also proposes an experimental model of an SS-WDM transmission system where one broadband ASE light source is shared between an optical transmission system and an optical sensor system (see Figs. 24 and 27). To ensure a more accurate comparison of its performance data, a simulation model is also developed, which is based on the selection of the elements of the experimental layout scheme. Unlike other research in this field, the author's goal is to achieve an error-free ($BER < 10^{-9}$) transmission system model that provides reliable output for both – the transmitted data channels and the optical sensor channels. In addition, the initial study uses a maximum bit rate of 1.5 Gbit/s for each channel, which was primarily limited by the light source characteristics described in the chapter's following subsections.

In addition, another simulation scheme of this type was implemented within the OptSim software to allow a more detailed performance comparison between the simulation and experimental scheme using a common broadband light source for a spectrally sliced data transmission system and an FBG optical sensor using a similar system architecture, as well as the use of optical elements and their parameters. Figure 24 shows the developed simulation model for the experimental scheme, which has 3 main parts CO, ODN, and ONT. In the central part of CO, the ASE source is selected as the source of the BLS. The optical band of the ASE source from 191.75 THz to 195.8 THz is used for the operation of the FBG optical sensor.

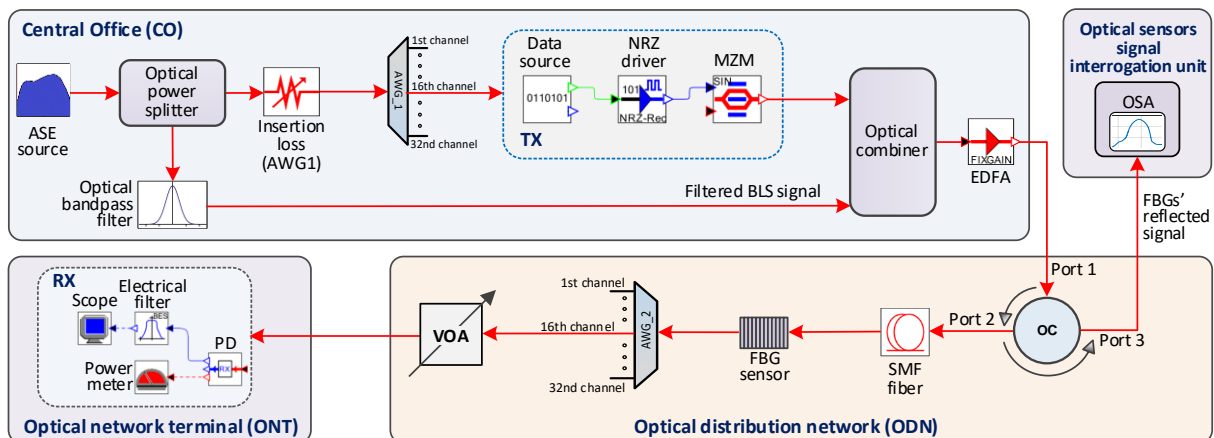


Fig. 24. The simulation model of 1.5 Gbit/s spectrum-sliced transmission system with embedded FBG sensor.

In this situation, several scenarios for one channel are tested. The data transfer bit rate is set to 1.5 Gbit/s. The signal quality is then measured as the BER difference (BER correlation diagrams) with or without an FBG optical sensor at a 20 km long fiber transmission line. Figure 25 shows the BER compared to the average received optical power for 1.5 Gbit/s signals after a 20 km long SMF fiber transmission line. The same configuration is then applied, but the 20 km long data transmission line is changed to non-data transmission line mode – back-to-back (B2B). Figure 26 shows BER correlation diagrams for B2B transmission.

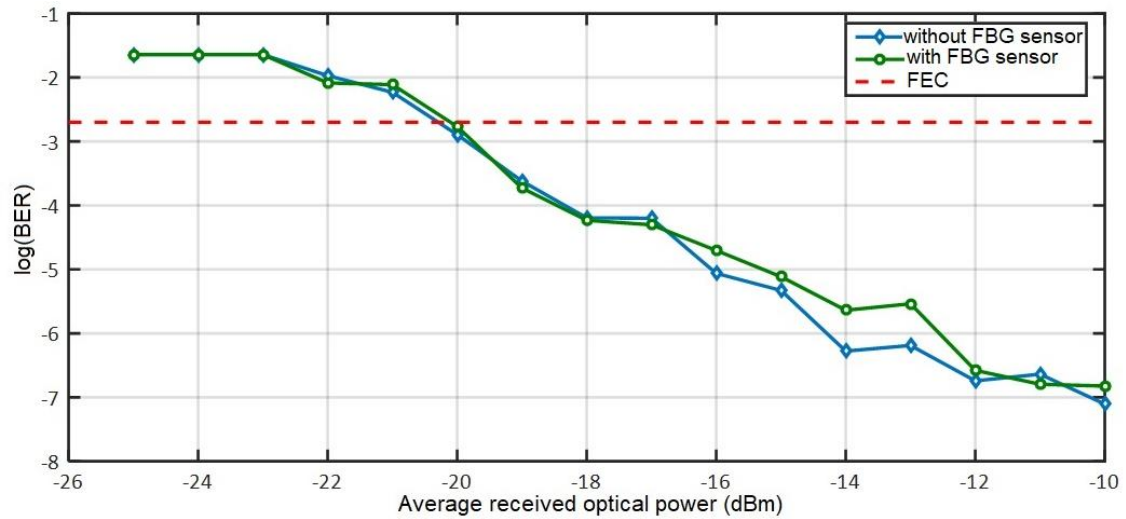


Fig. 25. BER compared to an average received optical power of 1.5 Gbit/s for spectrally sliced data signals after a 20 km SMF transmission line.

From the measured results (see Figs 25 and 26) the author calculates that for a system with B2B and 20 km long SMF fiber, the power penalty in the situation of cooperation of both systems is about 0.2 and 0.5 dB at FEC level 2×10^{-3} if a comparison with an optical transmission system without an integrated FBG optical sensor was performed. The power penalty (for a system with an FBG sensor) between a 20 km long optical transmission line and a B2B configuration at an FEC level of 2×10^{-3} is approximately 0.7 dB, which can be described as insignificant.

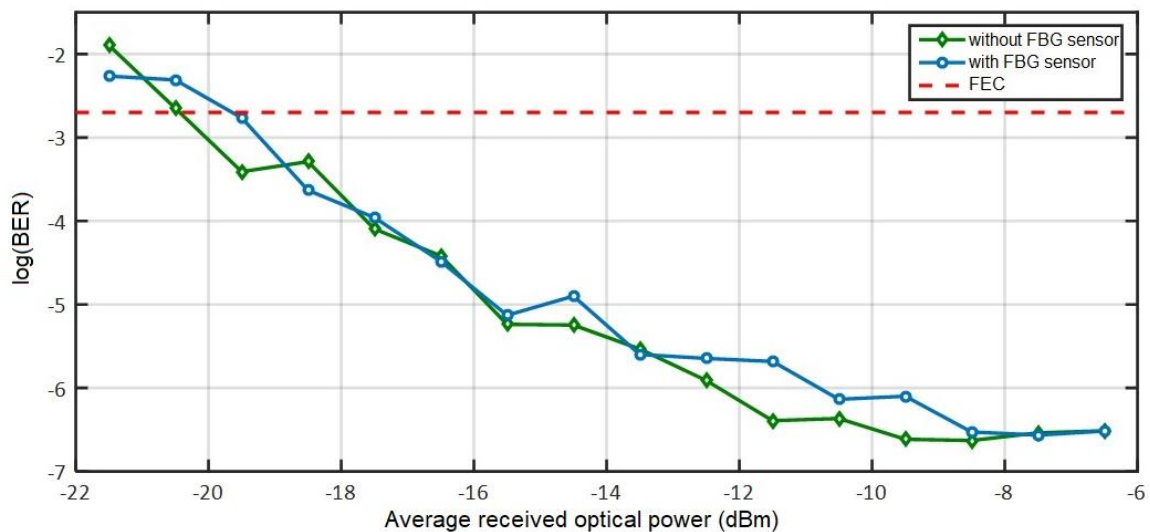


Fig. 26. BER compared to the average received optical power for 1.5 Gbit/s spectrally sliced data signals in a B2B transmission configuration.

An experimental optical fiber system, shown in Fig. 27, has been implemented in a study on the implementation of an efficient interaction for an optical transmission system with an embedded FBG sensor within one common optical fiber.

The main aspect of this system is that only one common BLS source is used for data transmission and sensor channels. It is important to emphasize that the same spectral characteristic curve of the FBG optical sensor is used in the implementation of the simulation and experimental systems.

The implemented WDM data transmission system is based on the spectral slicing of the BLS light source, namely, the broadband ASE light source. As an alternative to ASE, LEDs or

SLEDs, which typically have a higher output power, can be used in the implementation of spectrally sliced multi-channel transmission systems.

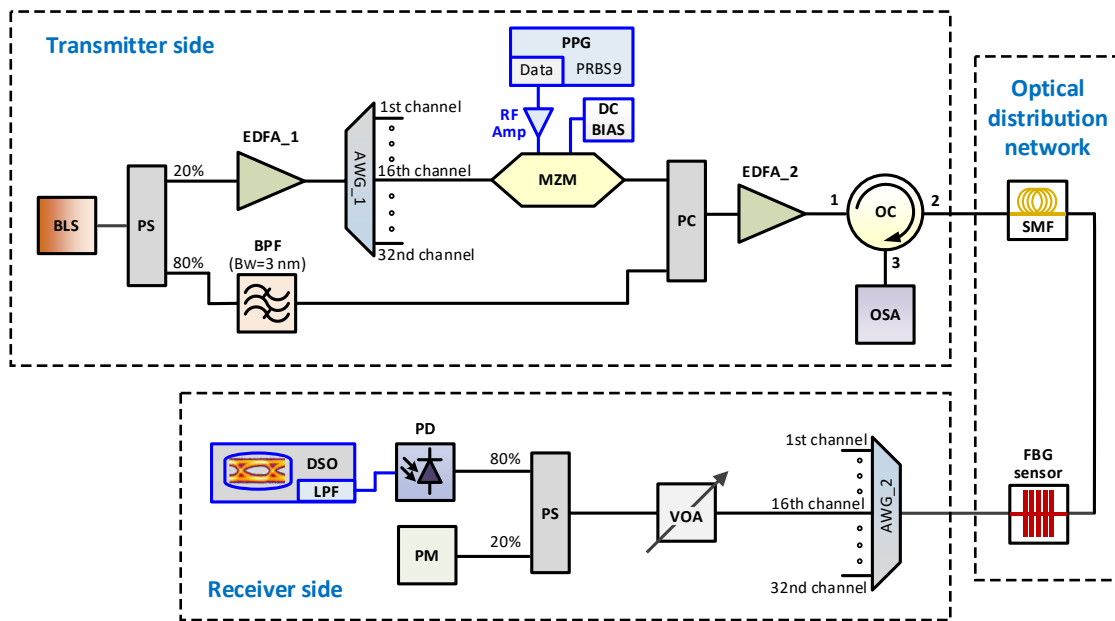


Fig. 27. Experimental system of spectrum-sliced WDM fiber optical transmission system with embedded FBG sensing system fed by a single shared broadband light source.

As can be seen in Fig. 28 (a) and (c), after 1.25 Gbit/s B2B configuration transmission, the received optical signal eye diagrams are widely open and the calculated BER = 4.6×10^{-16} , but after a 20 km long SMF fiber transmission line, the BER increases to 1.3×10^{-9} .

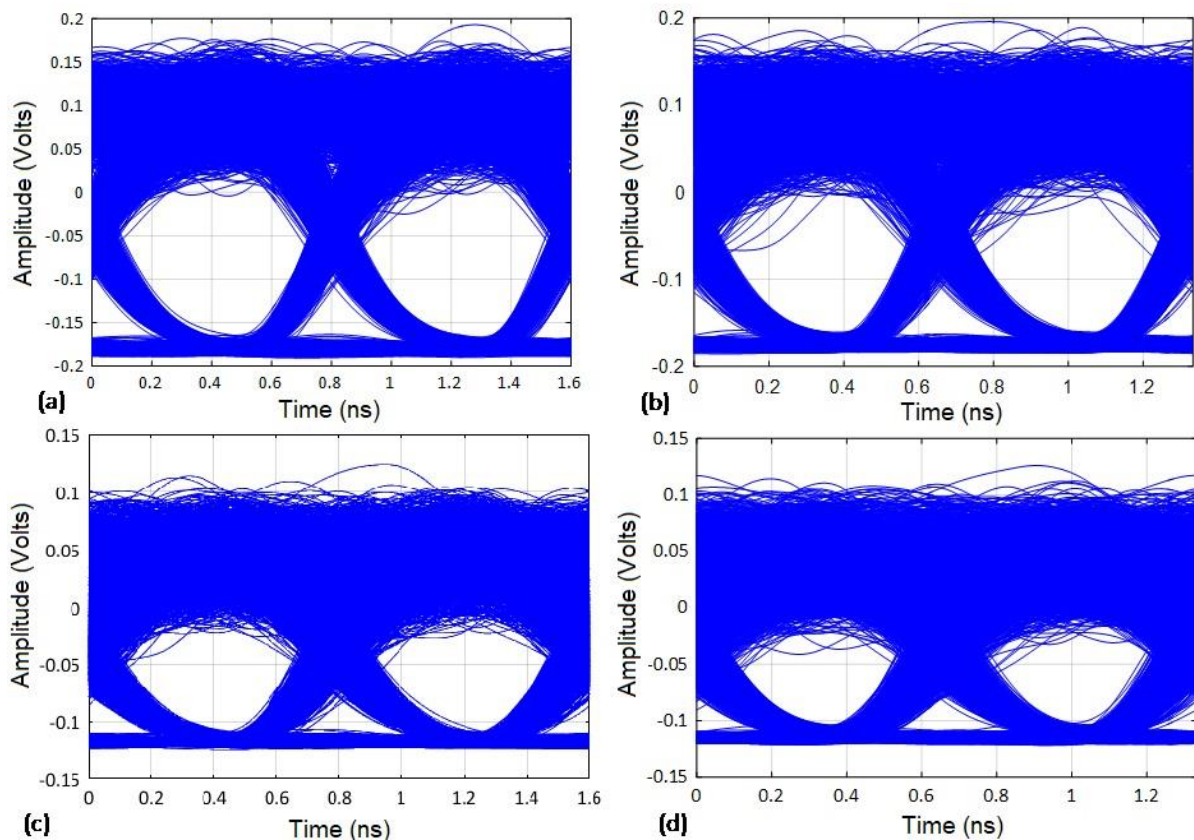


Fig. 28. Eye diagrams of received (a) 1.25 Gbit/s B2B signal; (b) 1.5 Gbit/s B2B signal; (c) 1.25 Gbit/s signal after 20 km transmission; and (d) 1.5 Gbit/s signal after 20 km transmission SMF fiber.

As shown in Figs. 28 (b) and (d), an increase in the bit rate from 1.25 Gbit/s to 1.5 Gbit/s leads to a decrease in the quality of the received signal. Numerically, the BER value in this situation according to the B2B configuration with a bit rate of 1.5 Gbit/s indicates that the BER of the received optical signal is 9.7×10^{-12} . However, after a 20 km long SMF fiber transmission line, it increased to BER 6.1×10^{-7} . It is important to understand that during data transmission, the transmitted signal is affected by the parallel transmitted FBG sensor signal from the BPF. The author estimated that the effect of this sensor's light source on the quality of the received signal was insignificant, because the spectral regions of the FBG and data channels did not overlap, and a sufficiently large spectral distance between data transmission channels and the optical sensor is provided.

From the obtained results (see Figs. 29 and 30), it was calculated that in the configuration of 1.5 Gbit/s bit rate, power penalty in the situation of 20 km long data transmission line, compared to B2B configuration measurements, at FEC level 2×10^{-3} is about 1.5 dB. The reason for this power penalty is mainly due to the noise type nature of the broadband ASE light source used, as well as the dispersion.

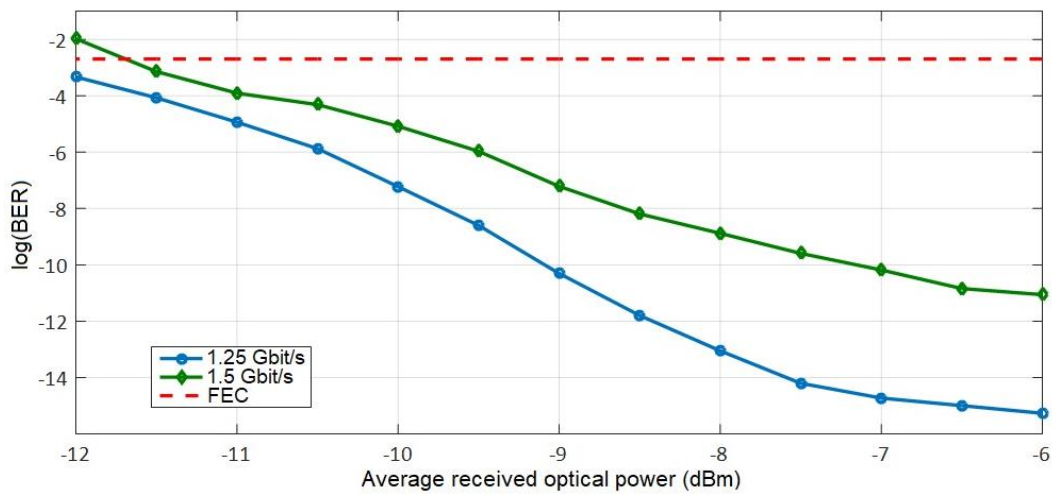


Fig. 29. BER compared to the average received optical power for 1.25 Gbit/s and 1.5 Gbit/s signals in B2B configuration transmission.

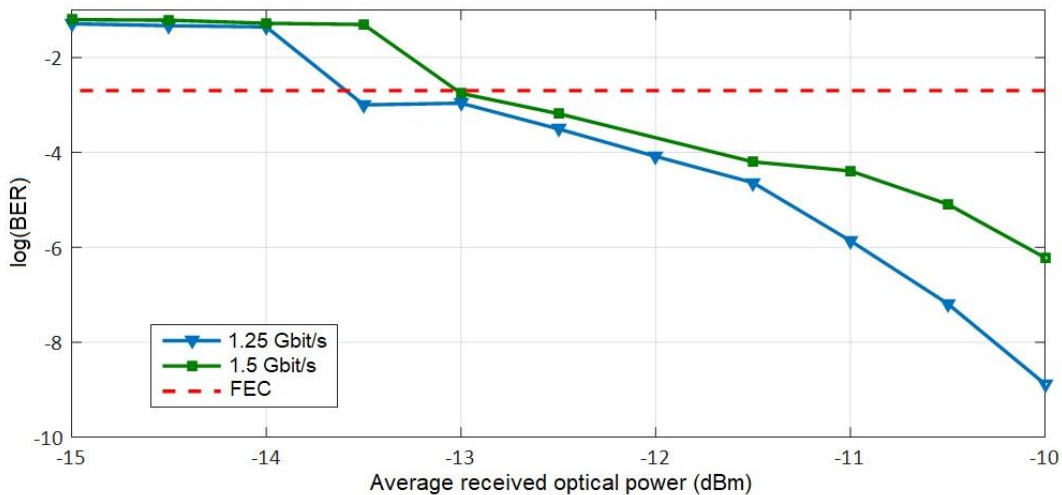


Fig. 30. BER compared to the average received optical power for 1.25 Gbit/s and 1.5 Gbit/s signals after a 20 km SMF transmission line.

As shown in Figs. 29 and 30, BER performance below the 7 % data overhead FEC limit of 2.3×10^{-3} is obtained in all data transmission scenarios with bit rates of 1.25 and 1.5 Gbit/s. Thus, transmission without significant errors is ensured, as well as the coexistence of data and sensor network in one common experimental system is realized.

MAIN RESULTS OF THE DOCTORAL THESIS

During the development of the Doctoral Thesis, the following **main conclusions** were obtained:

1. The developed hybrid system's model, which includes a network of 5 FBG fiber optic temperature sensors and 4 data channels, 10 Gbit/s WDM-PON fiber optic metro-access communication system, can provide at least 20 km long data transmission line operation with accepted received BER signal of $\leq 10^{-9}$, and determine the effect of the measured temperature on the variation of the reflected wavelength of the FBG optical sensors, which in this configuration is on average 1 GHz (8 pm) per 1 °C.
2. With the advanced precision FBG sensors' reflected signal spectral peak algorithm and mathematical equation developed in this work it is possible to calculate and estimate the FBG optical sensors theoretical channel spacing in the FBG sensors' network, which in the optical C-band (frequency range from 192 THz to 195.5 THz) is at least 207.746 GHz.
3. Using a single shared broadband light source, a combined spectrally sliced 1.5 Gbit/s 32 data channel WDM-PON transmission and FBG optical sensor network model can be created, providing the received BER of the data signal $\leq 9.7 \times 10^{-12}$ in B2B (no fiber optic line) configuration and $\text{BER} \leq 6.1 \times 10^{-7}$ in a 20 km long transmission line configuration.
4. Within one optical fiber, a model can be created in which a network of 5 FBG optical sensors is placed together with 8 WDM-PON 10 Gbit/s transmission data channels, between which a 2.5 Gbit/s 7 data channel system is visually hidden, ensuring adequate received signal quality ($\text{BER} \leq 7.16 \times 10^{-17}$ for the WDM-PON system and $\text{BER} \leq 1.11 \times 10^{-5}$ for the stealth data channel system) after a 20 km long fiber optic data transmission line.

The recommendations developed in the Doctoral Thesis are intended both for the improvement of the existing optical metro-access networks and for the introduction of new fiber optic transmission systems and sensor networks.

REFERENCES

- [1] Arena M., Viscardi M. Strain State Detection in Composite Structures: Review and New Challenges// *Journal of Composites Science*. 2020; 4(2):60. <https://doi.org/10.3390/jcs4020060>.
- [2] Bock W. J., Nawrocka M. S., Martynkien T., Urbanczyk W. and Demers S. A Fiber-Optic Temperature Sensor for Marine Applications// 2005 IEEE Instrumentation and Measurement Technology Conference Proceedings, Ottawa, Ont., 2005, pp. 1054–1056, DOI: 10.1109/IMTC.2005.1604302.
- [3] Bohnert K., Wildermuth S., Frank A., Brändle H. Fiber-optic voltage sensor using fiber gyro technology// *Procedia Engineering*, Volume 5, 2010, pp. 1091–1094, ISSN 1877-7058.
- [4] Bohnert K., Frank A., Müller G., Yang L., Lenner M., Gabus P., Gu X., and Marchese S. Fiber optic current and voltage sensors for electric power transmission systems// *Proc. SPIE 10654, Fiber Optic Sensors and Applications XV*, 1065402 (14 May 2018).
- [5] Chen Y. et al. Stealth transmission of 127-chip SSFBG EPS-TPE/D OOK-OCDM secure signal over a public 2-wavelength WDM network// *Proceedings of 2012 2nd International Conference on Computer Science and Network Technology*, Changchun, 2012, pp. 420–423.
- [6] Elayoubi K., Rissons A., Belmonte A., Optical test bench experiments for 1-Tb/s satellite feeder uplinks// *Laser Communication and Propagation through the Atmosphere and Oceans VII*, Aug 2018, San Diego, United States. pp. 1–12.
- [7] Fernandez-Valdivielso C., Matias I.R., Arregui F.J. Simultaneous measurement of strain and temperature using a fiber Bragg grating and a thermochromic material// 2002 15th Optical Fiber Sensors Conference Technical Digest. OFS 2002(Cat. No.02EX533), Portland, OR, USA, 2002, pp. 203–206 vol.1, DOI: 10.1109/OFS.2002.1000537.
- [8] Fiber-To-The-Home TOP 100 Broadband Communities Magazine, Fiber-to-the-home leaders and innovators for 2018, A BBC Staff Report, Jul. 2018.
- [9] Gao S., Ji C., Ning Q., Chen W., Li J. High-sensitive Mach-Zehnder interferometric temperature fiber-optic sensor based on core-offset splicing technique// *Optical Fiber Technology*, Volume 56, 2020, 102202, ISSN 1068-5200.
- [10] International Telecommunication Union (ITU), ITU-T PON standards — progress and recent activities, Q2/SG15. 1638 2019 Photonics & Electromagnetics Research Symposium – Fall (PIERS – FALL), Xiamen, China, 17–20 December.
- [11] ITU-T Recommendation G.694.1, Spectral grids for WDM applications: DWDM frequency grid, International Telecommunication Union, Telecommunication standardization sector of ITU, pp. 1–7, 2002.
- [12] ITU-T Recommendation G.975.1, Series G: Transmission systems and media, digital systems and networks, Digital sections and digital line systems – Optical fibre submarine cable systems, Forward error correction for high bit-rate DWDM submarine systems, International Telecommunication Union, Telecommunication standardization sector of ITU, pp. 1–58, 2004.
- [13] Jiang J. et al., Development of optical fiber temperature sensor for aviation industry// 2016 15th International Conference on Optical Communications and Networks (ICOON), Hangzhou, 2016, pp. 1–3, DOI: 10.1109/ICOON.2016.7875863.
- [14] Kottke C., Hilt J., Habel K., Vučić J. and Langer K. 1.25 Gbit/s visible light WDM link based on DMT modulation of a single RGB LED luminary// 2012 38th European Conference and Exhibition on Optical Communications, Amsterdam, 2012, pp. 1–3, DOI: 10.1364/ECEOC.2012.We.3.B.4.
- [15] Kravtsov K., Wu B., Glesk I., Prucnal P. R. and Narimanov E., Stealth Transmission over a WDM Network with Detection Based on an All-Optical Threshold// *LEOS 2007 –*

- IEEE Lasers and Electro-Optics Society Annual Meeting Conference Proceedings, Lake Buena Vista, FL, 2007, pp. 480–481.
- [16] Kumar R. et al. High sensitivity temperature sensor based on a polymer filled hollow core optical fibre interferometer// 2017 25th Optical Fiber Sensors Conference (OFS), Jeju, 2017, pp. 1–4, DOI: 10.1117/12.2265041.
- [17] Ledentsov Jr. N., Agustin M., Chorchos L., Kropp J.-R., Shchukin V. A., Kalosha V. P., Koepp M., Caspar C., Turkiewicz J. P., Ledentsov N. N. Energy efficient 850-nm VCSEL based optical transmitter and receiver link capable of 56 Gbit/s NRZ operation// Proc. SPIE 10938, Vertical-Cavity Surface-Emitting Lasers XXIII, 109380J (1 March 2019).
- [18] Marcelo M. Werneck, Regina C. S. B. Allil, Bessie A. Ribeiro and Fábio V. B. de Nazaré A Guide to Fiber Bragg Grating Sensors, Current Trends in Short- and Long-period Fiber Gratings, Christian Cuadrado-Laborde, IntechOpen, May 2013, DOI: 10.5772/54682.
- [19] Morana A. et al., Steady-state radiation-induced effects on the performances of BOTDA and BOTDR optical fiber sensors// IEEE Transactions on Nuclear Science, Vol. 65, No. 1, 111–118, Jan. 2018, DOI: 10.1109/TNS.2017.2772333.
- [20] Muciaccia T., Gargano F., Passaro V.M.N. Passive Optical Access Networks: State of the Art and Future Evolution// Photonics. 2014; 1(4): 323–346. <https://doi.org/10.3390/photonics1040323>.
- [21] Mukherjee B., Optical Metro Networks. In: Optical WDM Networks. Optical Networks. Springer, Boston, MA., 2006, https://doi.org/10.1007/0-387-29188-1_6
- [22] Poeggel S., Leen G., Bremer K. and Lewis E. Miniature Optical fiber combined pressure- and temperature sensor for medical applications// SENSORS, 2012 IEEE, Taipei, Taiwan, 2012, pp. 1–4, DOI: 10.1109/ICSENS.2012.6411305.
- [23] Prucnal P.R., Fok M.P., Deng Y. and Wang Z. Physical layer security in fiber optic networks using optical signal processing// 2009 Asia Communications and Photonics Conference and Exhibition (ACP), Shanghai, 2009, pp. 1–10.
- [24] Qu Y., Wang W., Peng J., Lv D., Dai J. and Yang M. Sensitivity-enhanced temperature sensor based on metalized optical fiber grating for marine temperature monitoring// 2017 16th International Conference on Optical Communications and Networks (ICO CN), Wuzhen, 2017, pp. 1–3, DOI: 10.1109/ICO CN.2017.8121293.
- [25] Rajan, G. (Ed.). (2015). Optical Fiber Sensors: Advanced Techniques and Applications (1st ed.). CRC Press. <https://doi.org/10.1201/b18074>.
- [26] Senkans U., Braunfelds J., Lyashuk I, Porins J., Spolitis S., Bobrovs V. Research on FBG-Based Sensor Networks and Their Coexistence with Fiber Optical Transmission Systems// Journal of Sensors, vol. 2019, Article ID 6459387, 13 p., 2019.
- [27] Silva R., Martins. H., Nascimento I, Baptista, J.M., Ribeiro A., Santos J., Jorge P., Frazão O. Optical Current Sensors for High Power Systems: A Review// MDPI, Applied Sciences, 2012, 2, 602–628; doi:10.3390/app2030602, ISSN 2076-3417.
- [28] Su G., et al. WDM Optical Steganography Based on Super-Continuum Light Source// 2019 18th International Conference on Optical Communications and Networks (ICO CN), Huangshan, China, 2019, pp. 1–3.
- [29] Tsai W. et al. A 20-m/40-Gb/s 1550-nm DFB LD-Based FSO Link// in IEEE Photonics Journal, vol. 7, no. 6, pp. 1–7, Dec. 2015, Art no. 7905907, DOI: 10.1109/JPHOT.2015.2506172.
- [30] Vučić J., Kottke C., Habel K., and Langer K. 803 Mbit/s visible light WDM link based on DMT modulation of a single RGB LED luminary// 2011 Optical Fiber Communication Conference and Exposition and the National Fiber Optic Engineers Conference, Los Angeles, CA, 2011, pp. 1–3.
- [31] Wilson B. A. and Blue T. E. Quasi-Distributed Temperature Sensing Using Type-II Fiber Bragg Gratings in Sapphire Optical Fiber to Temperatures up to 1300 °C// in IEEE Sensors Journal, vol. 18, no. 20, pp. 8345–8351, 15 Oct.15, 2018, DOI: 10.1109/JSEN.2018.2865910.

- [32] Yang M., Yang K., Tang J., Li C. and Shang F. High-sensitivity quasi-distributed temperature sensors based on weak FBGs Fabry-Perot structure with metal coating// 2017 16th International Conference on Optical Communications and Networks (ICOON), Wuzhen, 2017, pp. 1–3, DOI: 10.1109/ICOON.2017.8121290.
- [33] Zhang L., Shi B., Zeni L., Minardo A., Zhu H., and Jia L., An fiber Bragg grating-based monitoring system for slope deformation studies in geotechnical centrifuges// *Sensors*, Vol. 19, No. 7, 1591, 2019.
- [34] Zhang Y., Gao S., and Zhang A.P. Optically Heated Long-Period Grating as Temperature-Insensitive Fiber-Optic Refractive-Index Sensor// in *IEEE Photonics Journal*, vol. 4, no. 6, pp. 2340–2345, Dec. 2012, DOI: 10.1109/JPHOT.2012.2232907.
- [35] Zhigang C., Zhao Z., Xiaochun J., Tao S., Rui W., Chenchen Y., Shenglai Z., Liang L., Benli Y., Strain-insensitive and high temperature fiber sensor based on a Mach–Zehnder modal interferometer// *Optical Fiber Technology*, Volume 20, Issue 1, 2014, pp. 24–27, ISSN 1068-5200.
- [36] Britannica Bragg Law / Internets: <https://www.britannica.com/biography/Lawrence-Bragg>
- [37] Cisco Annual Internet Report (2018-2023) / Internets: <https://www.cisco.com/c/en/us/solutions/collateral/executive-perspectives/annual-internet-report/white-paper-c11-741490.html>
- [38] Cisco – Solutions for IP Optimized Optical transport / Internets: <https://www.cisco.com/c/en/us/products/optical-networking/white-paper-sp-ip-optimized-optical-transport.html>
- [39] Fabry-Perot Interferometers, RP Photonics Encyclopedia / Internets: https://www.rp-photonics.com/fabry_perot_interferometers.html
- [40] FTTH Council Europe – Panorama, Markets at September 2019 / Internets: <https://www.ftthcouncil.eu/documents/FTTH%20Council%20Europe%20-%20Panorama%20at%20September%202019%20-%20Webinar%20Version4.pdf>
- [41] Global Market Insights – Optical Sensor Market Size By Product / Internets: <https://www.gminsights.com/industry-analysis/optical-sensor-market>
- [42] Grand View Research – Distributed Fiber Optic Sensor Market Size Worth \$1.87 Billion By 2025 / Internets: <https://www.grandviewresearch.com/press-release/global-distributed-fiber-optic-sensor-sensing-dfos-market>
- [43] Spectrecolgy – Spectroscopy & Optical Sensing Solutions / Internets: <https://www.spectrecolgy.com/reflection/>